Journal of Medicinal Chemistry

Article

Optimizing Protonation States for Selective Double Strand DNA Photocleavage in Hypoxic Tumors: pH-Gated Transitions of Lysine Dipeptides

Kemal Kaya, Saumya Roy, Juan Carlos Nogues, Juan Camilo Rojas, Zlatko Sokolikj, Diego A. R. Zorio, and Igor V. Alabugin

J. Med. Chem., **Just Accepted Manuscript** • DOI: 10.1021/acs.jmedchem.6b01164 • Publication Date (Web): 15 Aug 2016

ACS Publications

Journal of Medicinal Chemistry is published by the American Chemical Society. 1155 Sixteenth Street N.W., Washington, DC 20036

Optimizing Protonation States for Selective Double Strand DNA Photocleavage in Hypoxic Tumors: pH-Gated Transitions of Lysine Dipeptides

Kemal Kaya[†,‡], Saumya Roy[†], Juan Carlos Nogues[†], Juan Camilo Rojas[†], Zlatko Sokolikj[†], Diego A. R. Zorio[§], Igor V. Alabugin[†*]

†*Department of Chemistry and Biochemistry, Florida State University, Tallahassee, FL 32306-4390, USA.*

‡ *Department of Chemistry, Dumlupınar University, Kütahya, 43100 Turkey*

§*Department of Biomedical Sciences, College of Medicine, Florida State University, Tallahassee, FL 32306, USA*

Abstract:

We report pH-switching properties of the new family of dipeptide-acetylene conjugates where pH-gated light-activated double strand (ds) DNA cleavage is controlled by variations in electronic and geometric parameters. The conjugates have higher activities at the slightly acidic pH values that separate normal and cancerous tissue (pH<7). This favorable pH dependence originates from several elements of structural design. Basicities of the two amines determine the threshold pH range where the changes in binding and reactivity are observed whereas the distance between the two amino groups and the hydrophobic aryl alkyne moiety can further modulate DNA binding. The changes of the protonation state from a neutral molecule to a dication results in dramatically increased efficiency of ds DNA photocleavage, the most therapeutically valuable type of DNA cleavage.

Introduction

The 2015 Nobel Prize in Chemistry illustrates the importance of mechanistic studies of DNA damage and repair. In human cells, a single double-strand (ds) DNA cleavage can potentially cause the loss of more than 100 million base pairs of genetic information.[1] Double stranded DNA cleavage, which is much more difficult to repair than single-strand (ss) DNA cleavage, is particularly beneficial for therapeutic purposes[2] since it leads to efficient self-programmed cell death (apoptosis). DNA damage can be achieved chemically[3] or photochemically[4] for cancer therapy.

Natural enediynes,[5] are self-defense tools for microorganisms that target DNA of competing species with astonishing efficiency.[6] The key feature of the enediyne molecules is ability to cause double stranded DNA (ds DNA) cleavage. For example, calicheamicin leads about 25% of ds DNA cleavage (~3:1 ss:ds ratio),[7] significantly overperforming such common ds-cleaving agents as bleomycins (ss:ds ratios of 6:1-20:1[8,9]). Upon activation of enediyne moiety, *p*-benzyne diradical is generated via Bergman cyclization.[10] This highly reactive diradical abstracts hydrogen atoms from DNA, initiating a sequence of further reactions that can culminate in ds DNA cleavage.[11] Unfortunately, the selectivity of these natural antibiotics towards cancer cells is low, rendering such compounds highly toxic towards healthy cells as well. Such indiscriminate toxicity calls for the incorporation of additional structural elements that introduce the required selectivity in this class of cytotoxic reagents. We have shown earlier that photochemical activation can be the source of such selectivity and that the DNA-damaging ability of enediynes can be replicated by photochemically activated

alkynes.[12] Furthermore, we found that the efficiency of such photodamage can be regulated by acidity of the media. [13]

Warburg has shown that cancer cells increase their production of lactic acid due to their faster metabolism. [14] The cell has a number of mechanisms for exporting H^+ ions to extracellular environment. However, drugs like amiloride,[15,16] nigericin[17] and hydralyzine can equilibrate the extracellular and extracellular H^+ ions concentration.[18,19] This process lowers the intracellular pH of cancer cells, thus differentiating tumors from the healthy tissues. One can take advantage of the acidic environment of cancer tissues by designing new chemical agents that selectively react at the lower pH of the tumors.[20,21] An attractive approach for optimizing the reactivity and selectivity of such compounds involves incorporation of basic amino acids.[22]

Lysine is an attractive amino acid for pH regulation due to the presence of two amino groups. When lysine's carboxylic group is used to connect this amino acid to a DNA-cleaving agent, both lysine's amino groups are preserved. The first[23, 24] and second-generation[25] of lysine enediynes, lysine mono acetylenes[26] and *meta*-diyne lysine conjugates[27] were synthesized to make pH-gated DNA-cleavage applicable to cancer therapy. The first generation of lysine conjugates was also shown to damage intracellular DNA and to display interesting selectivity for ds DNA cleavage, targeting G-sites flanking AT-tracks.[28] The two amino groups of all lysine conjugates have drastically different basicity – whereas the ε-amino group is protonated throughout the entire biologically relevant pH-region, α-amino group undergoes protonation at ~pH 7, the threshold that separates cancer from healthy tissues. The second generation probed for

the further control of efficiency by using different connections between two lysine residues.

Because the selectivity of DNA cleavage is controlled by the α-amino group of lysine, we decided to test whether DNA-cleavers with even higher selectivity toward cancer cells can be developed by redesigning the conjugates to possess only α-amino groups. For these new conjugates, the transition to acidic pH will transform *neutral* species directly to the *dicationic* form, potentially increasing the selectivity of the conjugates toward acidic cancer cells. We have also suggested that we can fine-tune the pH-dependence further by varying the distance between the two amino groups (Figure 1).

Figure 1: Left: Design of new amino acid-acetylene hybrids with variable distances between the two α-NH_2 groups. Right: the concept of pH-regulation of the DNA-cleaving activity of light-activated DNA cleaving agents.

If two amino groups are sufficiently close, they should affect each other's basicity. However, the degree of such interaction and its dependence on the spatial separation between the two bases are unknown. In order to probe this effect, we designed new dipeptides where the distance between α-amino groups is changed in a systematic way. We have also synthesized dipeptide conjugates where the two α-amino groups mimic the distance between the α - and ε- amino groups of lysine.

Results and Discussion

Synthesis

Peptide bond formation upon condensation with the carboxyl group of other amino acids converted the ε-amino group of lysine (**11**), δ-amino group of ornithine (**14**), and the β-amino group of alanine (**17**), into respective amides. Because these amides

were derived from amino acids, each of such transformation was equivalent to trading the terminal amino groups of the intermediate structure for an α-amino group in the final product, providing access to a family of alkyne dipeptide conjugates containing *two* α -NH_2 groups with the different degrees of spatial separation.

Scheme 1. Synthesis of designed hybrid molecules.

Boc-protected peptide conjugates (**12, 15** and **18**) were synthesized by coupling respective amines (**11, 14** and **17**) with α-amino Boc-protected amino acids (**9**) (glysine, alanine, phenylalanine and tryptophan) using dicyclohexylcarbodiimide (DCC) or 1-ethyl-3-(3-dimethylaminopropyl) carbodiimide (*EDCI*) / 1-hydroxybenzotriazole *(HOBt)* as coupling reagents. These peptides are then coupled to the DNA cleaver (**10**) after deprotection of methyl ester. Removal of the Boc-groups with trifluoroacetic acid (TFA) in CH_2Cl_2 produces the target compounds **1 – 8 (**Scheme 1**)**. The final products were fully characterized by spectroscopic methods and used in the DNA-photocleavage studies as TFA salts. The full list of compounds investigated in this work is given in Scheme 2.

Scheme 2. The structures of dipeptide-acetylene conjugates. A: Lysine bridge. B: Ornithine bridge. C: **α** -Amino alanine bridge.

Determination of pKa Values

NMR Titrations:

The α-amino groups control the selectivity of DNA-binding and cleaving by creating a number of available protonation states. Formation and interconversion of these states can be readily monitored by ^{1}H-NMR because protonation of amino groups strongly effects the chemical shift of α–C-H groups. By following the chemical shifts of

the respective protons, pKa values[29] of the individual amino group could be determined (Figure 2).

Scheme 3. The pK_a values obtained from ^1H NMR titration.

For the lysine-bridged conjugates **1** and **2** where the bridge between the two amino groups is relatively long (8 atoms), the difference between the basicity of these groups is relatively small. The pK_a differences of only 0.1 suggest that the two amines can be considered as independent functional groups. However, this model is likely to be an oversimplification because the titration curves clearly show that two α-amino groups are more basic (pK_a = 7.3 and 7.4) in **1** than in **2** (pK_a =6.6 and 6.7).[30] In other words, the terminal Ph group of **2** may impose an effect even at the remote amino group positioned at the center of the molecule. The origin of this interesting observation is unclear at the moment but one can suggest that it may be an indication of the contribution of a coiled conformation where the terminal Ph ring is brought to the proximity of the electron-deficient aromatic π-system of the DNA-photocleaving part by a combination of hydrophobic effect and π/π-interactions. If such conformational effect operates, it should have a consequence for the DNA binding where uncoiling of the more stable conformation will impose an additional penalty. If this is true, the protonation effect on binding of compound **2** (and its smaller analogue **6**) will be less pronounced in comparison to that in their analogues without the terminal Ph group. Interestingly, such behavior is indeed observed (vide infra).

In contrast, the two pK_a values of the ornithine-bridged compounds **4** (pK_a = 7.2, 7.7) and **5** (pK_a = 7.0, 7.8) are noticeably different (0.5-0.8 pK_a unit). This observation suggests that the two groups are sufficiently close in space, so the first group protonation

makes the second group protonation more difficult. However, behavior of the Ph-containing compound **6** is once again peculiar. Identical pK_as of 7.0 are found for both amines (Table 1). Again, this observation suggests that the conformational profile of the Ph-substituted conjugate is quite different from that of its cousins **4** and **5**. We could not determine the pK_a values of compound **3, 7** and **8** by NMR due to their lack of sufficient solubility in D_2O (Scheme 3). For these compounds, we had to turn to the significantly more sensitive measurements based on fluorescence quenching.

Figure 2. Chemical shift-pD titration plots for α-hydrogens in conjugates **2** and **3** (1 mM) in D_2O.

Fluorescence Titrations:

Fluorescence provides additional insight in the protonation states of α-amino groups because, upon excitation of the chromophore, the free lone pair of the amino group can quench excited state via intramolecular photoinduced electron transfer (PET). The quenching process is blocked when the amino groups are protonated and the donor lone pair of nitrogen is inaccessible. Changes in fluorescence intensity as a function of pH fit to the Henderson-Hasselbalch equation for acid-base equilibrium. Only amino groups that are spatially close to the chromophore quench its fluorescence efficiently. This spatial dependence accounts for the observation of only one pKa value for the conjugates **1-6** (Figure 3).

Figure 3. Selected pKa values obtained from fluorescence.

The difference between pK_as measured by NMR and fluorescence stems from the different electronic state of the interrogated molecule. The pK_a values obtained from

NMR is the acid dissociation constant of the ground state. However, the pK_a values from fluorescence reflect the excited state properties of the molecules. For most compounds, the pKas determined by the two methods are quite close, with the excited state pKa being slightly lower (i.e., amine is slightly less basic). The similarity is expected because the excitation is concentrated at the conjugated chromophore. The Ph-substituted conjugate **2** is again anomalous. Generally, only one pKa is observed corresponding to the spatially close ammonium moiety (excited states are short lived and less sensitive to the electronic properties of remote parts of the molecule). However, for the β-alanine conjugates **7** and **8** where the 2nd amino group is much closer to the chromophore, its protonation state can also be gauged by the fluorescence intensity change.

Table 1. Summary of pK_a values of the compounds.

The two acidities play complementary roles in achieving pH-gated selectivity of DNA cleavage. In particular, the ground state acidities are more important in DNA binding. When the cell has more acidic intracellular pH (cancer cells), the greater fraction of the compound will be bound to DNA. Thus, the acidic cancer tissues may be targeted more efficiently. On the other hand, excited state acidities are important for pH-gating by opening or shutting down the photochemical activation pathway responsible for the DNA damage. This is why we report both the ground state and the excited state acidities.

DNA Binding

(UV)

The interactions between DNA and our conjugates were analyzed by UV-Vis spectroscopy. The intrinsic DNA binding constants were calculated using the equation 1,[31]

$$[DNA]/(\varepsilon_a - \varepsilon_f) = [DNA]/(\varepsilon_b - \varepsilon_f) + 1/K_b(\varepsilon_b - \varepsilon_f) \qquad \textit{Equation 1}$$

where ε_a is the apparent extinction coefficient of complex with DNA, ε_b is the extinction coefficient of the fully bound complex, ε_f is the extinction coefficient of unbound compound, and K_b is the DNA binding constant of the compound. $[DNA]/(\varepsilon_a - \varepsilon_f)$ is plotted vs. [DNA] and slope is divided by *y*-intercept gave the (K_b) binding constant.

The results are summarized in Table 2. The measured DNA binding constants are comparable with those for the known DNA intercalators from the literature (10^5-10^{11} M^{-1}).[32] In every case, the binding constants slightly increase when pH increases - the trend similar to that in other lysine conjugates.[27] Although the increase in DNA binding at the lower pH was general, the magnitude of this increase varied for compounds of different nature. When pH increases, ammonium groups lose their charges and as a result, different binding interactions may become more important than electrostatic interactions with the backbone. For example, the hydrophobic part of the conjugates (the photocleaver) may approach one of the DNA grooves in order to get away from the aqueous environment. Indeed, the spectral information is consistent with changes of the binding modes.

The conjugates show strong absorption at ~310 nm. With the addition of DNA, the absorbance of the conjugates decreased with a concomitant small red shift, suggesting intercalative binding between DNA and conjugates. Whereas both a distinct isosbestic point and a red shift are clearly observed at pH 6, these spectral features disappear at pH 8 (Figure 5), suggesting switch to multiple binding modes at the higher pHs.

Table 2. DNA Binding constants from UV

The magnitudes of the pH-induced variations in binding depend on the substitution. Again, the Ph-substituted (Ph-Ala) conjugates **2, 6, 8** are anomalous - they show slightly

greater binding at pH 6 but also display a noticeably smaller increase at binding (5.7-, 3.0-, 1.1-fold, respectively) in comparison the Me-substituted (Ala) analogues **1,5,7** (10.5, 4.6-, 3.5-fold, respectively). The glycine analogue shows a >4-fold increase comparable to that for the alanine counterpart **5**, albeit with a slightly sharper increase at the pH 6/7 threshold. On the other hand, the tryptophane analogue **3** shows only a small 1.7 increase, even smaller than the increase in the related Ph-Ala compound **2**.

Figure 4. Absorption spectral changes of **1** (15 μM) on titration of CT DNA (0– 40 μM) in phosphate buffer (pH 6, pH 7 and pH 8).

EtBr Displacement:

The binding constants of the conjugates are comparable with the reported values for DNA intercalators in literature[31]. In order to better understand the DNA binding modes of the conjugates and the effects of varying pH on intercalation, we performed ethidium bromide (EtBr) displacement experiments. The results summarized in Table 3, show that all of the conjugates exhibited the most EtBr displacement capabilities at pH 6, decreasing displacement with increasing pH. The presence of the aromatic systems (phenyl ring on conjugate **2** and **6** and indole moiety on compouınd **3**) can lead to intercalation with DNA. Furthermore, Schneider et al. described earlier that such intercalation can be augmented by presence of a positive charge in the vicinity of an aromatic moiety assisted by the positively charged amino groups.[32] This structural feature suggests that these compounds can intercalate between DNA base pairs and displace the competitive DNA intercalator (EtBr).

Compounds **2** and **3** exhibited the largest drop in displacement when going from pH6 to pH7. This pH dependence is constant across all the conjugates and suggests interactions between our molecules and DNA increases at slightly acidic conditions, correlating with the observed increase in selectivity for double stranded cleavage of DNA by the conjugates under acidic conditions discussed below. It is important to consider the decrease in displacement and interactions at the neutral (pH7) and basic (pH8) conditions is influenced by the conjugate's transitions from di-cationic to neutral which partially dictates the affinity for the hydrophilic backbone of DNA vs the hydrophobic grooves, as well as their solubility. These results are consistent with findings in previous literature which correlate the increased displacement of the conjugates at pH 6 to protonated amino groups having increased interactions with the negative phosphate backbone of DNA[13].

Table 3. Stern-Volmer quenching constants of the compounds (**1**-**8**) from EtBr displacement.

DNA Photocleavage

The ability of dipeptide conjugates to cleave DNA upon irradiation was investigated using conversion of supercoiled plasmid DNA (Form I) into the respective circular (ss cleavage) and linear (ds cleavage) forms (Forms II and III, respectively). The relative amounts of the three DNA forms were determined by densitometric analysis of the gel electrophoresis bands. The lysine conjugates at 15 μM concentrations have shown a higher and more selective DNA-cleaving activity than conjugates that mimic lysine amino groups; With this in mind, we will focus the discussion below on compounds **1**, **2** and **3**.

Figure 5. Quantified cleavage data for plasmid relaxation assay for DNA photocleavage with 15 μM of acetylenic conjugates **1** (left), **2** (middle), **3** (right) and 38 μM (b.p.) of pBR322 plasmid DNA at pH range of 6 – 8 after 10 min. of UV (>300 nm) irradiation. Reported values represent the average of three experiments. Code: Form I, Blue; Form II, Red; Form III, Green.

The most remarkable observation is the selectivity of ds DNA cleavage induced by compound **2** when the pH changes from neutral to slightly acidic (pH 6). Even though the reactivity of compounds **1** and **3** is higher than compound **2**, the selectivity of compound **2** between pH 6 and pH 7 is much better, showing no ds DNA cleavage at pH 7 or pH 8. This result correlates with the basicity of the α-amino groups of compound **2** (pKa1=6.7 and pKa2=6.8). At pH 6, the dominant form of compound **3** is dicationic. At pH 7, the dominant form of compound **2** is likely nonprotonated. Considering electrostatic interactions, the binding affinity of compound **2** and DNA is stronger if these two α-amino groups are protonated.

Figure 6. Quantified cleavage data for plasmid relaxation assay for DNA photocleavage with 15 μM of acetylenic conjugates **4** (left), **5** (middle), **6** (right) and 38 μM (b.p.) of pBR322 plasmid DNA at pH range of 6 – 8 after 10 min. of UV (>300 nm) irradiation. Reported values represent the average of three experiments. Code: Form I, Blue; Form II, Red; Form III, Green.

In the case of ornithine conjugates **5**, **6** and **7**, the ability of the ds DNA cleavage is active at lower pH conditions (pH 6). However; the DNA cleavage at neutral pH (pH 7) and basic conditions (pH 8) is less pronounced. With alanine conjugates, the ds DNA photocleavage activity is lost.

Figure 7. Quantified cleavage data for plasmid relaxation assay for DNA photocleavage with 15 μM of acetylenic conjugates **7** (left) and **8** (right) and 30 μM (b.p.) of pBR322 plasmid DNA at pH range of 6 – 8 after 10 min. of UV (>300 nm) irradiation. Reported values represent the average of three experiments. Code: Form I, Blue; Form II, Red.

Statistical Studies

Further investigation on the origin of strand breaks prompts the question: Are ds DNA breaks coordinated or do they occur random due to multiple ss DNA breaks? To answer this question, we used the Freifelder–Trubo[33] ($\boldsymbol{n_2 = n_1^2(2h+1)/4L}$) equation. From this equation, n_2 (double strand breaks) values can be calculated by using typical n_1 (single strand breaks) values obtained from the each experiments. Assuming that the distribution of ds DNA breaks between individual follows a Poisson distribution,[34] we also calculated the Poisson distribution of strand cuts and average number of ss-(n_1) and ds-breaks (n_2) per DNA molecule using the equation $\boldsymbol{n_2 = 1/[(f_I + f_{II} + f_{III})/ f_{III} - 1]}$ and – $\boldsymbol{\ln f_I = n_1 + n_2 = n_{Tot}}$.

The DNA-photocleavage experiments were performed as a function of irradiation time at pH 6 for conjugates **1**, **2** and **3**. Quantified values from densitometry are shown in Table 4.

Figure 8. Quantified cleavage data for plasmid relaxation assay for DNA photocleavage with 15 μM of conjugates **1** (left), **2** (middle), **3** (right) and 30 μM (b.p.) of pBR322 plasmid DNA at pH range of 6 – 8 after 10 min. of UV (>300 nm) irradiation. Code: Form I, Blue; Form II, Red; Form III, Green.

Table 4. Statistical analysis of the single-strand and double-strand break formation by **1**, **2** and **3** as a function of irradiation time at pH 6.0.

Under these assumptions**,** n_1/n_2 is a good indicator for determining if cleavage occurs randomly or in a coordinated way. The observed n_1/n_2 ratio is at least 41 times greater (up to 140 times greater) than random Poisson distribution. Taking the average numbers, we can conclude that about 90% of ds DNA breaks produced by these compounds corresponds to the true ds-damage rather than to a combination of random ss DNA breaks.

Mechanistic Studies

In the absence of light, the conjugates do not induce ds DNA cleavage. Hence, DNA damage originates from the formation of excited state of the alkyne "warhead". Possible mechanisms[35] responsible for the observed photodamage include a variety of possibilities such as cross-link formation between dipeptides and DNA, oxidative damage through electron transfer from nucleobases,[36] alkylation of DNA,[45] hydrogen abstraction,[37,38] abasic site generation,[39] and reactive oxygen species (ROS).

Figure 9. Effect of hydroxyl radical/singlet oxygen scavengers (20 mM) upon the efficiency of DNA cleavage of compounds **1** (left), **2** (middle) and **3** (right) at pH 6 at 15 μM of compounds.

To investigate the effect of reactive oxygen species (ROS), we used the plasmid relaxation assays for the cleavage with compounds **1**, **2, 3** (Figure 9)**, 4, 5** and **6** (Figure 10) in the presence of hydroxyl radical (glycerol, DMSO)[40,41] and singlet oxygen (NaN_3)[42] scavengers.

Figure 10. Effect of hydroxyl radical/singlet oxygen scavengers (20 mM) upon the efficiency of DNA (30 μM b.p.) cleavage of compounds **4** (left), **5** (middle) and **6** (right) at pH 6 (20mM sodium phosphate buffer) at 15 μM of compounds.

Singlet oxygen and hydroxyl radical scavengers show no significant effect on the efficiency of DNA damage by compounds **3**, **4** and **5**. However, the DNA cleavage activity of the conjugates **5**, **6** and **7** is inhibited by sodium azide (NaN_3) and glycerol. In the case of conjugate **6** with DMSO, there is no inhibition from the scavenger on the ds DNA cleavage.

Abasic Site Generation:

Next question arises whether or not our conjugates are able penetrate the cell membrane, find the nuclei and break DNA inside the cell. To answer this question, we used the abasic site determination experiment to understand if our conjugates can function as DNA-photocleavers inside of the cell. Apurinic/apyrimidinic (AP) sites[43] result from the cleavage of *N*-glycosylic bond as a result of DNA damage[44] initiated by alkylation,[45] deamination[46] and the most frequently oxidation[47] of DNA bases. Oxidative damage is caused by reactive oxygen species (ROS), in particular, the hydroxyl radical. The results of AP site determination for conjugate **2** (the most selective compound) are shown in Figure 11. The graph also shows the internal standard points for certain numbers AP sites. The control experiment, that involves only UV irradiation, generates 10 abasic sites per 10^5 base pairs. However, conjugate **2** is able generate 17 AP sites when it is activated with UV light for 2 hrs. In other words, the amount of AP sites almost doubled in the presence of conjugates activated with light. Furthermore, these

experiments have also confirmed that our molecules (**1**, **2** and **3**) are able to penetrate cell membrane, find the nuclei and perform their DNA-cleaving function upon photochemical excitation.

Figure 11. Abasic Site Generation/Detection by the compound 2.

Conclusion

We have designed and prepared the third generation of acetylene-dipeptide conjugates. The conjugates change from neutral to *dicationic* under acidic conditions, making them selectively more reactive towards ds DNA in acidified conditions typical for cancerous tissue. Statistical analysis shows that the ds cleavage was caused by a coordinated ds cleavage event instead of two random ss cleavage events. Scavenger experiments have shown that there is no significant effect of reactive oxygen species on DNA damage. Furthermore, the conjugates are also able to penetrate the cell membrane and generate abasic sites in DNA.

Experimental Section

General information. ^{1}H, ^{13}C NMR spectra were collected on a Bruker 400 MHz and 600 MHz NMR spectrometer. Mass spectrometry data was collected on a Jeol JMS-600H. UV spectra were recorded on a Shimadzu UV-2100. Fluorescence spectra were obtained with SPEX FluoMax spectrofluorimeter using right-angle geometry. pH was adjusted with AB 15 plus pH meter (Accument) after standardization at 25 ºC. All buffers were prepared and pH-adjusted at room temperature (25°C). Purity of compounds is ≥95%.

Plasmid DNA Photocleavage. pBR322 plasmid DNA (4,361 b/p; from BioLabs Inc., 1μg/μL solution in 10 mM Tris-HCl (pH 8.0), and 1mM EDTA buffer) was diluted to a concentration of 0.01 μg/μL. The solution containing cleavage agent, DNA (30 μM/bp) in 20 mM sodium phosphate buffer was incubated for 1 hour at 30 ^{o}C. Samples were placed on ice at a distance of 20 cm from 200 W Hg-Xe lamp (Spectra-Physics, Laser & Photonics Oriel Instruments with long pass filter with 324 nm cut-on wavelength).

Electrophoretic Analysis. The gel electrophoresis was carried out in 1x TBE buffer at 80 V using Miligel FisherBiotech Horizontal Electrophoresis System. All gels were run on 1% agarose slab gels. Before loading, the DNA samples were mixed with 0.33 volume of tracking dye containing bromophenol blue (0.25%) and glycerol (30%) in water. After staining in ethidium bromide solution (2 μg/ml) for 1 hour, the gel was washed with water and pictures were taken. The relative quantities of the supercoiled, nicked, and linear DNA were calculated by integrating the "area" of each spot by the image analyzer software Total/Lab (Nonlinear Dynamics Ltd., UK). The amount of supercoiled DNA was multiplied by factor of 1.4 to account for reduced ethidium bromide intercalation into supercoiled DNA.

Spectrometric determinations of pK_a. pH of 10 μM of compound solution in H_2O was adjusted with 10, 100 mM HCl (aq) and NaOH (aq) solution under nitrogen purged condition. Excitation wavelength was 330 nm and polymethacrylate fluorimeter cuvettes were used.

AP Site Determination. Human malignant melanoma cell line A375 (CRL-1619™) was obtained from the American Type Culture Collection (ATCC®). The cell line was cultured in RPMI 1640 medium supplemented with 10% fetal bovine serum (FBS) and

penicillin/streptomycin (Life Technologies®). Cells were propagated according to ATCC® guidelines and maintained in a 37 °C incubator with 5% CO_2 atmosphere. Cells (8×10^5) were plated in 10 cm cell culture dishes. Twenty-four hours later, 3 μM of compounds were added to cells and incubated for 1 h. Treated and untreated cells were exposed to UV radiation for 20 min and harvested at different time points post UV radiation. DNA from harvested cells was extracted using GeneElute Mammalian Genomic DNA kit (cat. no. G1N70, Sigma-Aldrich) and concentration was determined using NanoDrop™ Lite Spectrophotometer 1000 (Thermo Fisher Scientific). Abasic Sites (AP sites) counting was determined by following manufacturer's instructions for the DNA Damage Quantification Kit-AP Site Counting- (Cat#DK02) from Dojindo Molecular Technologies, Inc.

Analytical data of compounds

(S)-2,6-Diamino-*N*-((S)-5-amino-6-oxo-6-((4-((perfluoropyridin-4 yl)ethynyl)phenyl)amino)hexyl)hexanamide bis-trifluoroacetic acid salt (1): Boc-protected compound **13a** (193 mg, 0.29 mmol) was dissolved in CH_2Cl_2 (4 mL) and trifluoroacetic acid (4 mL) added. Reaction mixture was stirred for 4 h and concentrated in vacuo. Anhydrous diethyl ether (15 mL) were added to the crude product, solid immediately came out. The solid material was washed with anhydrous diethyl ether (3 × 10 mL) then chloroform (3 × 10 mL) to get pure TFA-salt in 53% yield. ^{1}H NMR (400 MHz, CD_3OD): 7.78 (d, J = 7.9 Hz, 2H), 7.64 (d, J = 7.9 Hz, 2H), 4.04 (t, J = 6.5 Hz, 1H), 3.86 (q, J = 7.3 Hz, 1H), 3.28 – 3.15 (m, 2H), 2.07 – 1.88 (m, 2H), 1.66 – 1.55 (m, 2H), 1.54 – 1.47 (m, 2H), 1.43 (d, J = 7.3 Hz, 2H); ^{13}C NMR (150 MHz, CD_3OD): δ 173.7, 171.5, 147.7 (d, J = 250 Hz), 145.7 (d, J = 272 Hz), 144.1, 109.8, 76.5, 57.7, 52.8,

42.6, 34.8, 32.4, 25.7, 20.2; HRMS (ESI): calcd for $C_{22}H_{23}F_4N_5O_2$ $[M + Na]^+$ 488.16856, found 488.16839.

(S)-2-amino-6-((S)-2-amino-3-phenylpropanamido)-N-(4-((perfluoropyridin-4-yl)ethynyl)phenyl)hexanamide Tri-trifluoroacetic acid salt (2): The compound **2** was prepared by using the same procedure as synthesis of compound **1** in 82% yield. ^{1}H NMR (400 MHz, CD_3OD): 7.76 (d, J=8.3 Hz, 2H), 7.58 (d, J=8.3 Hz, 2H), 7.35-7.27 (m, 3H), 7.23 (d, J=7.4, 2H), 4.01 (t, J=6.2 Hz, 1H), 3.97 (t, J=7.4 Hz, 1H), 3.27-3.24 (m, 1H), 3.11-3.07 (m, 2H), 3.01-2.97 (m, 1H),1.96-1.90 (m, 2H), 1.49-1.36 (m, 4H); ^{13}C NMR (150 MHz, CD_3OD): δ 169.9, 168.9, 145.6 (t, J=14.0 Hz), 144.2-143.9 (m), 142.4 (d, J=35.6 Hz) 141.5, 135.7, 134.3, 130.5, 130.1, 128.8, 121.1, 117.4, 107.2, 74.0, 55.9, 55.1, 40.0, 38.9, 32.3, 29.9, 23.2; HRMS (ESI+): calcd for $C_{28}H_{27}F_4N_5O_2H$ $[M + H]^+$ 542.21791, found 542.21994.

(S)-2,6-Diamino-*N*-((S)-5-amino-6-oxo-6-((4-((perfluoropyridin-4-yl)ethynyl)phenyl)amino)hexyl)hexanamide Tri-trifluoroacetic acid salt (3): The compound **3** was prepared by using the same procedure as synthesis of compound **1** in 41% yield. ^{1}H NMR (400 MHz, CD_3OD): 7.73 (d, J = 8.9 Hz, 2H),7.58 (d, J=7.6 Hz, 1H), 7.53 (d, J = 8.9 Hz, 2H), 7.36 (d, J = 8.4, 1H), 7.16 (s, 1H), 7.11 (dd, J = 8.4, 7.1 Hz, 1H), 7.03 (dd, J = 7.6, 7.1 Hz, 1H), 4.02 – 3.96 (m, 2H), 3.28 – 3.03 (m, 4H), 1.99 – 1.82 (m, 2H), 1.48 – 1.32 (m, 4H); ^{13}C NMR (150 MHz, CD_3OD): δ 170.4, 169.3, 145.1 (d, J = 254 Hz), 143.1 (d, J = 265 Hz), 141.5, 134.2, 128.5 122.9, 121.2, 120.2, 119.2, 117.3, 112.6, 108.3, 107.2, 73.9, 66.9, 55.3, 40.1, 32.4, 29.6, 29.1, 23.1, 15.4 ; HRMS (ESI): calcd for $C_{30}H_{28}F_4N_6O_2Na$ $[M + Na]^+$ 603.21076, found 603.20992.

(S)-2-amino-5-(2-aminoacetamido)-N-(4-((perfluoropyridin-4-yl)ethynyl)phenyl)pentanamide bis(2,2,2-trifluoroacetate) (4): The compound **4** was prepared by using the same procedure as synthesis of compound **1** in 78% yield. ^{1}H NMR (600 MHz, CD_3OD): 7.78 (d, *J* = 8.6 Hz, 2H), 7.64 (d, *J*=8.6 Hz, 2H), 4.06 (t, *J* = 6.4 Hz, 1H), 3.66 (s, 2H), 2.05 – 1.92 (m, 2H), 1.71-1.66 (m, 2H); ^{13}C NMR (150 MHz, CD_3OD): δ 168.7, 167.5, 163.1 (q, *J*=35 Hz), 144.9 (d, *J*=215 Hz), 143.3 (d, *J*=251 Hz), 141.4, 134.3, 121.0, 118.3, 117.5, 107.1, 74.0, 54.9, 41.4, 39.8, 30.1, 26.0; HRMS (ESI): calcd for $C_{20}H_{19}F_4N_5O_2H$ $[M + H]^+$ 438.15531, found 438.15530.

(S)-2-amino-5-((S)-2-aminopropanamido)-N-(4-((perfluoropyridin-4-yl)ethynyl)phenyl)pentanamide bis(2,2,2-trifluoroacetate) (5): The compound **5** was prepared by using the same procedure as synthesis of compound **1** in 85% yield. ^{1}H NMR (600 MHz, CD_3OD): 7.78 (d, *J* = 8.0 Hz, 2H), 7.64 (d, *J*=8.0 Hz, 2H), 4.06 (t, *J* = 6.0 Hz, 1H), 3.88 (q, J=6.7 Hz, 1H), 2.03 – 1.93 (m, 2H), 1.71-1.66 (m, 2H), 1.47 (d, *J* = 6.9 Hz, 3H);^{13}C NMR (150 MHz, CD_3OD): δ 171.3, 168.8, 163.1 (q, *J*=35 Hz), 144.9 (d, *J*=215 Hz), 144.0 (d, *J*=264 Hz), 141.5, 134.2, 121.0, 118.8 (d, J=125 Hz), 117.4, 107.2, 74.0, 54.8, 50.2, 39.8, 30.0, 25.8, 17.7; HRMS (ESI+): calcd for $C_{21}H_{21}F_4N_5O_2H$ $[M + H]^+$ 452.17096, found 452.17061.

(S)-2-amino-5-((S)-2-amino-3-phenylpropanamido)-N-(4-((perfluoropyridin-4-yl)ethynyl)phenyl)pentanamide bis(2,2,2-trifluoroacetate) (6): The compound **6** was prepared by using the same procedure as synthesis of compound **1** in 89% yield. ^{1}H NMR (600 MHz, CD_3OD): 7.79 (d, *J* = 8.6 Hz, 2H), 7.62 (d, *J*=8.7 Hz, 2H), 7.30-7.20 (m, 5H), 4.06 (t, *J* = 6.3 Hz, 1H), 4.02 (t, *J* = 7.4 Hz, 1H), 3.26-3.17 (m, 2H), 3.13 (dd, *J*=13.7Hz, J=7.3 Hz, 1H), 3.03-2.99 (m, 1H), 1.89 (q, *J*=7.6 Hz, 2H), 1.63-1.54 (m, 2H); ^{13}C NMR

(150 MHz, CD_3OD): δ 169.9, 168.7, 163.1 (q, *J*=34 Hz), 144.9 (d, *J*=215 Hz), 144.0 (t, *J*=263 Hz), 143.3 (d, *J*=251 Hz), 141.5, 135.6, 134.2, 130.4, 130.0, 128.8, 121.0, 119.2, 118.3, 117.4, 107.1, 74.0, 55.9, 54.7, 39.7, 38.8, 29.9, 25.5; HRMS (ESI): calcd for $C_{27}H_{25}F_4N_5O_2H$ $[M + H]^+$ 528.20226, found 528.20168.

(S)-2-amino-3-((S)-2-aminopropanamido)-N-(4-((perfluoropyridin-4-yl)ethynyl)phenyl)propanamide bis(2,2,2-trifluoroacetate) (7): The compound **7** was prepared by using the same procedure as synthesis of compound **1** in 88% yield. ^1H NMR (400 MHz, CD_3OD): 7.78 (d, *J*=8.7 Hz, 2H), 7.56 (d, *J*=8.7 Hz, 2H), 4.20 (t, *J*=4.8Hz, 1H), 3.95 (q, *J*=7.0Hz, 1H), 3.82 (dq, *J*=14.6 *J*=4.0Hz, 2H), 1.47 (d, *J*=7.0Hz, 3H); ^{13}C NMR (150 MHz, CD_3OD): δ 172.8, 166.7, 163.3, 145.7 (d, *J*=14 Hz), 144.8 (d, *J*=208 Hz), 143.2 (d, *J*=231 Hz), 141.4, 134.2, 121.2, 118.3, 117.5, 107.1, 74.0, 55.3, 50.2, 41.2, 17.4; HRMS: calcd for $C_{19}H_{17}F_4N_5O_2Na$ $[M + Na]^+$ 446.12161, found 446.12178.

(S)-2-amino-N-((S)-2-amino-3-oxo-3-((4-((perfluoropyridin-4-yl)ethynyl)phenyl)amino)propyl)-3-phenylpropanamide bis(2,2,2-trifluoroacetate) (8): The compound **8** was prepared by using the same procedure as synthesis of compound **1** in 84% yield. ^1H NMR (600 MHz, CD_3OD): 7.78 (d, *J*=8.7 Hz, 2H), 7.63 (d, *J*=8.6 Hz, 2H), 7.36-7.26 (m, 5H), 4.17 (t, *J*=5.5 Hz, 1H), 4.12 (dd, *J*=9.1 Hz *J*=5.6 Hz, 1H), 3.83 (dd, *J*=14.6 Hz *J*=5.8 Hz, 1H), 3.74 (dd, *J*=14.6 *J*=5.2 Hz, 1H), 3.24 (dd, *J*=14.3 *J*=5.5 Hz, 1H), 2.96 (dd, *J*=14.3 *J*=9.2 Hz, 1H); ^{13}C NMR (150 MHz, CD_3OD): δ 171.5, 166.7, 163.3 (q, *J*=35 Hz), 144.9 (d, *J*=217 Hz), 144.1 (t, *J*=247 Hz), 144.0 (d, *J*=26 Hz), 141.4, 135.5, 134.2, 130.4, 130.1, 128.9, 121.2, 116.9, 118.2 (d, J=293 Hz), 117.5, 107.2, 74.0, 55.8, 55.2, 41.2, 38.5; HRMS: calcd for $C_{25}H_{21}F_4N_5O_2Na$ $[M + Na]^+$ 522.15291, found 522.15258.

(S)-methyl2-((tert-butoxycarbonyl)amino)-6-((S)-2-((tert-butoxycarbonyl)amino)propanamido)hexanoate (12a): To a solution of Boc-protected acid, Boc-L-Ala-OH (**9b**) (400 mg, 2.11 mmol) in CH_2Cl_2 (15 mL) at 0 °C, EDCI (506 mg, 2.64 mmol) and HOBt (356 mg, 2.64 mmol) were added sequentially. After 20 min, the mixture of amine Lys(N-α-Boc)-OMe (**11**) (458 mg, 1.76 mmol) and DIPEA(0.9 mL, 5.28 mmol) were added to the reaction mixture. After stirring for 12 h at room temperature, the reaction mixture was extracted with ethyl acetate, washed with saturated NH_4Cl solution, water, brine, dried (Na_2SO_4), filtered, and concentrated in vacuo. Chromatographic purification (SiO_2, 40 % ethyl acetate in hexane eluant) of the residue provided dipeptide compound **12a** in 46 % yield. ^{1}H NMR (400 MHz, $CDCl_3$): δ 6.23 (bs,1H), 5.16 (bs, 1H), 5.05(bs,1H), 4.24(bs, 1H), 4.17 – 4.04 (m,1H), 3.73 (s,1H), 3.33 – 3.14 (m, 2H), 1.85 – 1.72 (m, 1H), 1.71 – 1.48 (m, 5H), 1.46 – 1.41 (m, 18H), 1.34 (d, J = 7.3 Hz, 3H); ^{13}C NMR (100 MHz, $CDCl_3$): δ 173.3, 172.9, 155.5, 155.4, 79.4, 60.2, 53.2, 52.0, 49.8, 38.6, 31.7, 28.2, 22.4, 18.5; HRMS (ESI): calcd for $C_{20}H_{37}N_3O_7Na$ $[M + Na]^+$ 454.25292, found 454.25280.

(S)-methyl 2-((tert-butoxycarbonyl)amino)-6-((S)-2-((tert-butoxycarbonyl)amino)-3-phenylpropanamido)hexanoate (12b): The compound **12b** was prepared by using the same procedure as synthesis of compound **12a** in 51% yield. ^{1}H NMR (600 MHz, $CDCl_3$): 7.31-7.18 (m, 5H), 5.81 (bs, 1H), 5.14 (bs, 2H), 4.27 (bs, 1H), 4.22 (bs, 1H), 3.73 (s, 3H), 3.14 (bs, 2H), 3.07-3.00 (m, 2H), 1.73 (bs, 1H), 1.63-1.56 (m, 1H), 1.44 (s, 9H), 1.40 (s, 9H), 1.37 (bs, 2H), 1.24 (bs, 2H); (150 MHz, $CDCl_3$): δ 173.4, 171.3, 155.6, 137.0, 129.4, 128.8, 127.1, 80.3, 80.1, 56.2, 53.4, 52.4, 39.0, 38.8, 32.2, 29.0, 28.5, 28.4, 22.6; HRMS (ESI+): calcd for $C_{26}H_{41}N_3O_7Na$ $[M + Na]^+$ 530.28422, found 530.28421.

(S)-methyl 2-((tert-butoxycarbonyl)amino)-6-((S)-2-((tert-butoxycarbonyl)amino)-3-(1H-indol-3-yl)propanamido)hexanoate (12c): The compound **12c** was prepared by using the same procedure as synthesis of compound **12a** in 41% yield. ^{1}H NMR (400 MHz, $CDCl_3$): δ 8.9 (bs, 1H), 7.67 (d, J = 7.5 Hz, 1H), 7.39 (d, J = 8.1 Hz, 1H), 7.19 (dd, J = 7.5,7.1 Hz, 1H), 7.04(s, 1H), 5.56 (bs, 1H), 5.21 (s, 1H), 5.10 (s, 1H), 4.43 (bs, 1H), 4.25 – 4.15 (m, 1H), 3.73 (s, 3H), 3.39 (d, J = 9.0 Hz, 1H), 3.15 – 3.02 (m, 3H), 1.73 – 1.55(m, 2H), 1.49(s, 9H), 1.45(s, 9H), 1.32 – 0.97, (m, 4H); ^{13}C NMR (100 MHz, $CDCl_3$): 173.1, 171.6, 155.5, 155.3, 136.1, 127.2, 123.2, 121.6, 119.1, 118.4, 111.2, 109.9, 77.8, 55.2, 53.2, 51.9, 38.6, 31.7, 28.1, 22.3; HRMS (ESI): calcd for $C_{28}H_{42}N_4O_7Na$ $[M + Na]^+$ 569.29512, found 569.29517.

(S)-methyl 2-*N*-[(1S)-5-[[(2S)-2,6-bis(*tert*-butoxycarbonylamino)hexanoyl]amino]-1-[[4-[2-(2,3,5,6-tetrafluoro-4-pyridyl)ethynyl]phenyl]carbamoyl]pentyl]carbamate (13a): The dipeptide **12a** (320 mg, 0.74 mmol) was dissolved in THF:MeOH:H_2O (3:1:1, 10 mL) at 0 °C. Then, $LiOH{\cdot}H_2O$ (93 mg, 2.22 mmol) was added and stirred at the room temperature for 3 h. The reaction mixture was then acidified to pH 2 with 1N HCl. It was extracted with ethyl acetate, washed with brine, dried (Na_2SO_4), filtered, and concentrated in vacuo to get the crude acid and used for further reaction. The prepared acid was dissolved in CH_2Cl_2 (10 mL) and cooled to 0 °C. It was sequentially treated with DCC (229 mg, 1.11 mmol) and HOBt (149 mg, 1.11 mmol). After 15 min, amine (**10**), (237 mg, 0.89 mmol) was added to the reaction mixture and stirred for 24 h, raising the temperature to rt. The reaction mixture was extracted with ethyl acetate, washed with saturated NH_4Cl solution, saturated $NaHCO_3$, 1 N HCl, water, brine, dried (Na_2SO_4), filtered, and concentrated in vacuo. Chromatographic purification (SiO_2, 60 % ethyl

acetate in hexane eluant) of the residue provided compound **13a** in 42 % yield. ^{1}H NMR (400 MHz, $CDCl_3$): δ 9.28 (bs, 1H), 7.64 (d, J = 6.9 Hz, 2H), 7.53 (d, J = 6.9 Hz, 2H), 6.77 (bs, 1H), 5.78 (bs, 1H), 5.31 (bs, 1H), 4.31 – 4.16 (m, 2H), 3.36 (s, 1H), 3.13 (s, 1H), 1.92 – 1.78 (m, 1H), 1.77 – 1.67 (m, 1H), 1.58 – 1.39 (m, 20H), 1.38 (d, J = 7.3 Hz, 2H^{13}C NMR (150 MHz, CD_3OD): δ 173.5, 171.7, 156.3, 155.8, 143.3 (d, J = 250 Hz), 141.5 (d, J = 280 Hz), 140.3, 133.2, 119.5, 117.3, 115.3, 107.0, 80.3, 73.1, 55.2, 50.0, 38.5, 31.5, 28.9, 28.3, 22.7, 18.6; HRMS (ESI): calcd for $C_{32}H_{39}F_4N_5O_6Na$ $[M + Na]^+$ 688.27342, found 688.27351.

{5-(2-tert-Butoxycarbonylamino-3-phenyl-propionylamino)-1-[4-(2,3,5,6-tetrafluoro-pyridin-4-ylethynyl)-phenylcarbamoyl]-pentyl}-carbamic acid tert-butyl ester (13b): The compound **13b** was prepared by using the same procedure as synthesis of compound **13a** in 35% yield. ^{1}H NMR (400 MHz, CD_3CN): 8.92 (bs, 1H), 7.71 (d, J=8.6 Hz, 2H), 7.59-757 (m, 2H), 7.30-7.19 (m, 5H), 6.72 (t, J= 5.5 Hz, 1H), 5.79 (d, J=7.1 Hz, 1H), 5.50 (d, J=7.1 Hz, 1H), 4.18 (dd, J=7.4, 1H), 4.04 (bs, 1H), 3.16-3.04 (m, 3H), 2.78 (dd, J=13.6,8.9, 1H), 1.78-1.63 (m, 2H), 1.40 (s, 11H), 1.33 (s, 11H); ^{13}C NMR (400 MHz, CD_3CN): δ 172.7, 172.6, 156.8, 156.3, 142.0, 145.8-143.0 (m), 138.7, 134.1, 130.2, 129.2, 127.5, 120.4, 115.7, 107.3, 80.1, 79.9, 79.1, 73.6, 56.9, 56.6, 38.9, 31.9, 29.6, 28.5, 28.4, 23.4; HRMS (ESI+): calcd for $C_{38}H_{43}F_4N_5O_6Na$ $[M + Na]^+$ 764.30472, found 764.30374.

(S)-methyl 2-*N*-[(1S)-5-[[(2S)-2,6-bis(*tert*-butoxycarbonylamino)hexanoyl]amino]-1-[[4-[2-(2,3,5,6-tetrafluoro-4-pyridyl)ethynyl]phenyl]carbamoyl]pentyl]carbamate (13c): The compound **13c** was prepared by using the same procedure as synthesis of compound **13a** in 38% yield. ^{1}H NMR (400 MHz, $CDCl_3$): δ 9.07 (bs, 1H), 8.79 (d, J =

6.9 Hz, 1H), 7.66 (d, *J* = 7.7 Hz, 1H), 7.56(d, J = 8.1 Hz, 1H), 7.36 (d, J = 8.1 Hz, 1H), 7.19 (dd, J = 7.7, 7.1 Hz, 1H), 7.11 (dd, J = 8.1, 7.1 Hz, 1H), 6.06 (s, 1H), 5.95 (bs, 1H), 5.42 (bs, 1H), 5.27 (bs, 1H), 4.45 (bs, 1H), 4.06 (bs,1H) 3.51 – 3.41 (m, 1H), 3.32 – 2.96 (m, 3H), 1.96 – 1.88 (m, 1H), 1.85 – 1.53 (m, 5H), 1.48 (s, 9H), 1.43 (s, 9H); ^{13}C NMR (150 MHz, $CDCl_3$): δ 169.2, 168.8, 153.9, 153.2, 141.0 (d, J = 270 Hz), 139.2(d, J = 250 Hz), 137.7, 133.8, 130.8, 124.9, 120.9, 119.6, 117.1, 116.2, 115.0, 113.2, 108.8, 107.9, 104.3, 78.2, 77.7, 52.9, 52.5, 35.9, 28.9, 26.1, 23.8, 23.0, 22.4, 19.9; HRMS (ESI): calcd for $C_{40}H_{44}F_4N_6O_6Na$ $[M + Na]^+$ 803.31561, found 803.31332.

(S)-methyl2-((tert-butoxycarbonyl)amino)-5-(2-((tert-butoxycarbonyl)amino)acetamido)pentanoate (15a): To a solution of Boc-protected acid, Boc-Gly-OH (**9a**) (285 mg, 1.63 mmol) in CH_2Cl_2 (15 mL) at 0 °C, EDCI (391 mg, 2.04 mmol) and HOBt (276 mg, 2.04 mmol) were added sequentially. After 20 min, the mixture of amine Boc-Orn-OMe (**14**) (335 mg, 1.36 mmol) and DIPEA (0.7 mL, 4.08 mmol) were added to the reaction mixture. After stirring for 12 h at room temperature, the reaction mixture was extracted with ethyl acetate, washed with saturated NH_4Cl solution, water, brine, dried (Na_2SO_4), filtered, and concentrated in vacuo. Chromatographic purification (SiO_2, 50 % ethyl acetate in hexane eluant) of the residue provided dipeptide compound **15a** in 49% yield. ^{1}H NMR (400 MHz, $CDCl_3$): 6.46 (bs, 1H), 5.27 (bs, 1H), 5.18 (d, *J* = 7.6 Hz, 1H), 4.28 (d, *J* =5.2 Hz, 1H), 3.76 (d, *J*= 5.6 Hz, 2H), 3.72 (s, 3H), 3.29 (q, *J*=6.2 Hz, 2H), 1.85-1.76 (m, 1H), 1.67-1.56 (m, 3H), 1.44 (s, 9H), 1.42 (s, 9H); ^{13}C NMR (100 MHz, CD_3OD): δ 173.1, 169.7, 156.3, 155.6, 80.3, 80.2, 53.2, 52.5, 44.5, 39.0, 30.3, 28.4, 25.6; HRMS (ESI+): calcd for $C_{18}H_{33}N3O_7Na$ $[M + Na]^+$ 426.22162, found 426.22159.

(S)-methyl2-((tert-butoxycarbonyl)amino)-5-((S)-2-((tert-butoxycarbonyl)amino)propanamido)pentanoate (15b): The compound **15b** was prepared by using the same procedure as synthesis of compound **15a** in 72% yield. ^{1}H NMR (600 MHz, $CDCl_3$): 6.40 (bs, 1H), 5.14 (d, *J* = 6.7 Hz, 1H), 5.03 (bs, 1H), 4.28 (d, *J* = 5.2 Hz, 1H), 4.11 (bs, 1H), 3.73 (s, 3H), 3.34-3.22 (m, 2H), 1.82 (bs, 1H), 1.66-1.54 (m, 3H), 1.44 (s, 18H), 1.34 (d, *J* = 7.1 Hz, 3H); (150 MHz, $CDCl_3$): δ 173.1, 173.0, 155.6, 80.0, 53.2, 52.4, 50.2, 38.9, 30.1, 28.4, 25.6, 18.7; HRMS (ESI+): calcd for $C_{19}H_{35}N_3O_7Na$ $[M + Na]^+$ 440.23727, found 440.23652.

(S)-methyl 2-((tert-butoxycarbonyl)amino)-5-((S)-2-((tert-butoxycarbonyl)amino)-3-phenylpropanamido)pentanoate (15c): The compound **15c** was prepared by using the same procedure as synthesis of compound **15a** in 75% yield. ^{1}H NMR (400 MHz, $CDCl_3$): 7.31-7.18 (m, 5H), 5.97 (bs, 1H), 5.08 (bs, 1H), 5.07 (bs, 1H), 4.28-4.19 (m, 2H), 3.73 (s, 3H), 3.18 (d, *J* = 3.6 Hz, 2H), 3.07-2.98 (m, 2H), 1.44 (s,11H), 1.40 (s, 11H;); ^{13}C NMR (100 MHz, $CDCl_3$): δ 173.0, 171.5, 155.5, 136.9, 129.3, 128.5, 126.8, 79.9, 55.9, 53.1, 52.2, 38.9, 29.9, 29.6, 28.3, 28.2, 25.4; HRMS (ESI+): calcd for $C_{25}H_{39}N_3O_7Na$ $[M + Na]^+$ 516.26857, found 516.26663.

{4-(2-tert-Butoxycarbonylamino-acetylamino)-1-[4-(2,3,5,6-tetrafluoro-pyridin-4-ylethynyl)-phenylcarbamoyl]-butyl}-carbamic acid tert-butylester (16a): The compound **16a** was prepared by using the same procedure as synthesis of compound **13a** in 22% yield. ^{1}H NMR (600 MHz, $CDCl_3$): 9.25 (bs, 1H), 7.71 (d, *J* = 8.6 Hz, 2H), 7.56 (d, *J*=8.6 Hz, 2H), 6.70 (bs, 1H), 5.38 (d, *J*=8.6 Hz, 1H), 5.26 (bs, 1H), 4.52 (bs, 1H), 3.84 (d, J=4.9Hz, 2H), 3.68 (bs, 1H), 3.30 (bs, 1H), 1.81 (bs, 1H), 1.66-1.59 (m, 3H),

1.45 (s, 9 H), 1.41 (s, 9H); HRMS (ESI+): calcd for $C_{30}H_{35}F_4N_5O_6Na$ $[M + Na]^+$ 660.24212, found 660.24018.

(1-{4-(3,3-Dimethyl-butyrylamino)-4-[4-(2,3,5,6-tetrafluoro-pyridin-4-ylethynyl)-phenylcarbamoyl]-butylcarbamoyl}-ethyl)-carbamic acid tert-butyl ester (16b): The compound **16b** was prepared by using the same procedure as synthesis of compound **13a** in 24% yield. ^{1}H NMR (600 MHz, $CDCl_3$): 9.31 (bs, 1H), 7.75 (d, *J* = 8.1 Hz, 2H), 7.57 (d, *J*=8.3 Hz, 2H), 6.67 (bs, 1H), 5.37 (d, *J* = 7.5 Hz, 1H), 4.90 (bs, 1H), 4.57 (bs, 1H), 4.13 (t, *J* = 6.6 Hz, 1H), 3.78 (bs, 1H), 3.16 (bs, 1H), 1.72 (bs, 2H), 1.58 (bs, 2H), 1.44 (s, 9H), 1.38 (d, *J* = 6.8 Hz, 3H), 1.33 (s, 9H); NMR (150 MHz, $CDCl_3$): δ 174.5, 171.5, 156.4, 155.9, 143.9 (d, *J* = 229 Hz), 142.8 (t, *J* = 262 Hz), 140.8, 133.5, 119.4, 117.8, 115.5, 107.2, 80.7, 80.2, 73.3, 53.3, 50.9, 37.8, 30.7, 28.5, 28.3, 26.1, 18.3; HRMS (ESI+): calcd for $C_{31}H_{37}F_4N_5O_6Na$ $[M + Na]^+$ 674.25777, found 674.25669.

{4-(2-tert-Butoxycarbonylamino-3-phenyl-propionylamino)-1-[4-(2,3,5,6-tetrafluoro-pyridin-4-ylethynyl)-phenylcarbamoyl]-butyl}-carbamic acid tert-butyl ester (16c): The compound **16c** was prepared by using the same procedure as synthesis of compound **13a** in 33% yield. ^{1}H NMR (600 MHz, $CDCl_3$): 9.28 (bs, 1H), 7.73 (d, *J* = 8.5 Hz, 2H), 7.58 (d, *J*=8.5 Hz, 2H), 7.31-7.18 (m, 5H), 6.23 (bs, 1H), 5.32 (d, *J* = 7.7 Hz, 1H), 4.96 (bs, 1H), 4.55 (bs, 1H), 4.26 (q, *J* = 7.2 Hz, 1H), 3.71 (bs, 1H), 3.10-3.07 (m, 1H), 3.04 (bs, 2H), 1.65-1.58 (m, 2H), 1.56-1.49 (m, 2H), 1.45 (s, 9H), 1.29 (s, 9H); ^{13}C NMR (150 MHz, $CDCl_3$): δ 173.0, 171.4, 156.4, 155.7, 143.6 (d, *J*=215 Hz), 143.5 (d, *J*=281 Hz), 142.8 (d, *J*=262 Hz), 140.8, 136.4, 133.5, 129.3, 128.9, 127.3, 119.4, 117.8, 115.5, 107.1, 80.7, 80.2, 73.3, 56.6, 53.3, 38.7, 37.9, 30.5, 28.5, 28.2, 26.0; HRMS (ESI+): calcd for $C_{37}H_{41}F_4N_5O_6Na$ $[M + Na]^+$ 750.28907, found 750.28720.

(S)-methyl2-((tert-butoxycarbonyl)amino)-3-((S)-2-((tert-butoxycarbonyl)amino)propanamido)propanoate (18a): To a solution of Boc-protected acid, Boc-Ala-OH (**9b**) (150 mg, 0.79 mmol) in CH_2Cl_2 (8 mL) at 0 °C, EDCI (189 mg, 0.99 mmol) and HOBt (134 mg, 0.99 mmol) were added sequentially. After 20 min, the mixture of amine (N-Boc-β-amino)-Ala-OMe (**17**) (144 mg, 0.66 mmol) and DIPEA (0.3 mL, 1.98 mmol) were added to the reaction mixture. After stirring for 12 h at room temperature, the reaction mixture was extracted with ethyl acetate, washed with saturated NH_4Cl solution, water, brine, dried (Na_2SO_4), filtered, and concentrated in vacuo. Chromatographic purification (SiO_2, 50 % ethyl acetate in hexane eluant) of the residue provided dipeptide compound **18a** in 84% yield. ^{1}H NMR (400 MHz, $CDCl_3$): 6.94 (bs, 1H), 5.68 (d, *J*=7.6 Hz, 1H), 5.18 (bs, 1H), 4.35 (bs, 1H), 4.10 (q, *J*=6.9 Hz, 1H), 3.71 (s, 3H), 3.60 (q, *J*=5.6 Hz, 2H), 1.42 (s, 9H), 1.40 (s, 9H), 1.30 (d, J=7.0Hz, 3H);); ^{13}C NMR (100 MHz, $CDCl_3$): δ 173.7, 171.3, 155.7, 80.2, 53.8, 52.7, 50.3, 41.4, 28.4, 28.3, 18.3; HRMS: calcd for $C_{17}H_{31}N_3O_7Na$ $[M + Na]^+$ 412.20597, found 412.20647.

(S)-methyl 2-((tert-butoxycarbonyl)amino)-3-((S)-2-((tert-butoxycarbonyl)amino)-3-phenylpropanamido)propanoate (18b): The compound **18b** was prepared by using the same procedure as synthesis of compound **18a** in 81% yield. ^{1}H NMR (600 MHz, $CDCl_3$): 7.31-7.18 (m, 5H), 6.42 (bs, 1H), 5.40 (d, *J*=6.3Hz 1H), 4.98 (bs, 1H), 4.29 (bs, 2H), 3.73 (s, 3H), 3.57 (bs, 2H), 3.08-2.98 (m, 2H), 1.43 (s, 9H), 1.40 (s, 9H); ^{13}C NMR (150 MHz, CD_3OD): δ 172.2, 171.3, 155.7, 136.7, 129.4, 128.9, 127.2, 80.5, 80.4, 56.1, 53.6, 52.8, 41.6, 38.3, 28.4, 28.3; HRMS: calcd for $C_{23}H_{35}N_3O_7Na$ $[M + Na]^+$ 488.23727, found 488.23631.

{2-(2-tert-Butoxycarbonylamino-propionylamino)-1-[4-(2,3,5,6-tetrafluoro-pyridin-4-ylethynyl)-phenylcarbamoyl]-ethyl}-carbamic acid tert-butyl ester (19a): The compound **19a** was prepared by using the same procedure as synthesis of compound **13a** in 19% yield. ^{1}H NMR (600 MHz, $CDCl_3$): 9.42 (bs, 1H), 7.62 (d, *J*=8.0 Hz, 2H), 7.56 (d, *J*=8.6 Hz, 2H), 7.11 (bs, 1H), 6.16 (bs, 1H), 5.03 (bs, 1H), 4.38 (bs, 1H), 4.09 (t, *J*=6.6, 1H), 3.92 (bs, 1H), 3.52 (bs, 1H), 1.46 (s, 9H), 1.37 (s, 9H), 1.369 (s, 3H); ^{13}C NMR (150 MHz, $CDCl_3$): δ 174.5, 169.6, 157.1, 155.9, 142.7 (t, *J*=253 Hz), 141.7 (d, *J*=263 Hz), 140.1, 133.5, 119.8, 117.6 (d, *J*= 16 Hz), 116.1, 106.9, 81.0, 80.8, 73.5, 55.6, 51.3, 41.1, 28.4, 28.3, 18.1; HRMS (ESI+): calcd for $C_{29}H_{33}F_4N_5O_6Na$ $[M + Na]^+$ 646.22647, found 646.22471.

(1-{2-tert-Butoxycarbonylamino-2-[4-(2,3,5,6-tetrafluoro-pyridin-4-ylethynyl)-phenylcarbamoyl]-ethylcarbamoyl}-2-phenyl-ethyl)-carbamic acid tert-butyl ester (19b): The compound **19b** was prepared by using the same procedure as synthesis of compound **13a** in 21% yield. ^{1}H NMR (600 MHz, $CDCl_3$): 9.32 (bs, 1H), 7.60-7.56 (m, 4H), 7.29-7.18 (m, 5H), 6.83 (bs, 1H), 5.99 (bs, 1H), 4.94 (d, *J*=4.1Hz 1H), 4.29 (d, *J*=6.1Hz 1H), 4.27 (bs, 1H), 3.92 (bs, 1H), 3.48 (bs, 1H), 3.11 (dd, *J*=13.8Hz, *J*=6.1Hz 1H), 2.99 (dd, *J*=13.9Hz, *J*=7.7Hz 1H), 1.48 (s, 9H), 1.34 (s, 9H); ^{13}C NMR (150 MHz, $CDCl_3$): δ 173.2, 169.5, 157.2, 155.8, 144.4 (d, *J*= 13 Hz), 142.8 (t, *J*=260 Hz), 142.7 (d, *J*=47 Hz), 140.9 (d, *J*=7 Hz), 140.1, 136.2, 133.5, 129.2, 129.1, 127.4, 119.7, 117.7 (d, *J*= 16 Hz), 116.1, 106.9, 81.2, 80.9, 73.5, 56.6, 55.7, 40.8, 38.2, 28.5, 28.3; HRMS: calcd for $C_{35}H_{37}F_4N_5O_6Na$ $[M + Na]^+$ 722.25777, found 722.25920.

Ancillary Information

Supporting Information

UV-Vis spectra, fluorescence data, AP site graphs, ^{1}H and ^{13}C NMR spectroscopic data for compounds. This material is available free of charge via the Internet at http:// pubs.acs.org

Corresponding Author Information

Igor V. Alabugin

Address:Department of Chemistry and Biochemistry, Florida State University, Tallahassee, FL 32306-4390, USA.

Email: alabugin@chem.fsu.edu

Phone: (850) 644 5795

Abbreviations Used

ds, double stranded; ss single stranded; AT-Tracks, adenosine thymidine-tracks; G-site, guanosine site; DIPEA, N,N-Diisopropylethylamine; DCC, dicyclohexylcarbodiimide; EDCI, 1-Ethyl-3-(3-dimethylaminopropyl)carbodiimide; HOBt, hydroxybenzotriazole; D_2O, deuterium oxide; NaN_3, sodium azide; R^2, coefficient of determination; pD, -log[deuterium ion]; TFP, tetrafluoropyridinyl; PET, photoinduced electron transfer; K_a, acid dissociation constant; K_b, DNA binding constants; CT DNA, calf thymus DNA; EtBr, ethidium bromide; K_{sv}, Stern-Volmer quenching constants; Form I, super coiled DNA plasmid/unreacted DNA; From II, circular DNA with single stranded cleavage; Form III, linear DNA with double stranded cleavage; b.p., base pair; n_1, number of single strand breaks; n_2, number of double strand breaks; n_{Tot}, total number of breaks; AP, apurinic/apyrimidinic

References

1. Helleday, T.; Lo, J.; van Gent, D. C.; Engelward, B. P. DNA double-strand break repair: from mechanistic understanding to cancer treatment. *DNA Repair* **2007**, *6*, 923-935.

2. Weaver, D. T. Regulation and repair of double-strand DNA breaks. *Crit. Rev. in Eukaryotic Gene Expression* **1996**, *6*, 345-375.

3. Stanulla, M.; Wang, J.; Chervinsky, D. S.; Thandla, S.; Aplan, P. D. DNA cleavage within the MLL breakpoint cluster region is a specific event which occurs as part of higher-order chromatin fragmentation during the initial stages of apoptosis. *Mol. Cell. Biol.* **1997**, *17*, 4070-4079.

4. Armitage, B. Photocleavage of Nucleic Acids. *Chem. Rev*. **1998**, *98*, 1171-1200.

5. Nicolaou, K. C.; Smith, A. L.; Yue, E. W. Chemistry and biology of natural and designed enediynes. *Proc. Natl. Acad. Sci. U. S. A.* **1993**, 90, 5881-5888.

6. Galm, U.; Hager, M. H.; Van Lanen, S. G.; Ju, J.; Thorson, J. S.; Shen, B. Antitumor antibiotics: bleomycin, enediynes, and mitomycin. *Chem. Re*v. **2005**, *105*, 739-758.

7. Elmroth, K.; Nygren, J.; Martensson, S.; Ismail, I. H.; Hammarsten, O. Cleavage of cellular DNA by calicheamicin gamma1. *DNA Repair* **2003**, *2*, 363-374.

8. (a) Povirk, L. F.; Wubker, W.; Kohnlein, W.; Hutchinson, F. DNA double-strand breaks and alkali-labile bonds produced by bleomycin. *Nucleic Acids Res.* **1977**, *4*, 3573-3580. (b) Charles, K.; Povirk, L. F. Action of Bleomycin on structural mimics of intermediates in DNA double-strand cleavage. *Chem. Res. Toxicol.* **1998**, *11*, 1580-1585.

9. (a) Lloyd, R. S.; Haidle, C. W.; Hewitt, R. R. Bleomycin-induced alkaline-labile damage and direct strand breakage of PM2 DNA, *Cancer Res.* **1978**, *38*, 3191-3196. (b)

Harsch, A.; Marzilli, L. A.; Bunt, R. C.; Stubbe, J.; Vouros, P. Accurate and rapid modeling of iron-bleomycin-induced DNA damage using tethered duplex oligonucleotides and electrospray ionization ion trap mass spectrometric analysis. *Nucleic Acids Res.* **2000**, *28*, 1978-1985. (c) Stubbe, J.; Kozarich, J. W. Mechanisms of bleomycin-induced DNA degradation. *Chem. Rev.* **1987**, *87*, 1107-1136. (d) Burger, R. M., Cleavage of nucleic acids by Bleomycin, *Chem. Rev.* **1998**, *98*, 1153-1170. (e) Hecht, S. M., Bleomycin: New perspectives on the mechanism of action, *J. Nat. Prod.* **2000**, *63*, 158-168. (f) Standke, K. H. C.; Brunnert, H., The estimation of affinity constants for the binding of model peptides to DNA by equilibrium dialysis. *Nucleic Acids Res.* **1975**, *2*, 1839-1850. (g) Ahmad, J.; Ashok, B. T.; Ali, R. Detection of oxidative DNA damage by a monoclonal antibody: role of lysyl residues in antigen binding. *Immun. Lett.* **1998**, *62*, 87. (h) Tyler, J. K.; Allen, K. E.; Everett, R. D. Mutation of a single lysine residue severely impairs the DNA recognition and regulatory functions of the VZV gene 62 transactivator protein. *Nucleic. Acids Res.* **1994**, *22*, 270-278.

10. (a) Bergman, R. G. Reactive 1,4-Dehydroaromatics. *Acc. Chem. Res.* **1973**, *6*, 25-31. (b) Mohamed, R. K.; Peterson, P. W.; Alabugin, I. V. Concerted reactions that produce diradicals and zwitterions: Electronic, steric, conformational and kinetic control of cycloaromatization processes. *Chem. Rev*. **2013**, *113*, 7089–7129.

11. For potential limitations/diversions of intermolecular H-atom transfer, see: (a) Baroudi, A.; Mauldin, J.; Alabugin, I. V. Conformationally gated fragmentations and rearrangements promoted by interception of the bergman cyclization through intramolecular H-abstraction: A possible mechanism of auto-resistance to natural enediyne antibiotics? *J. Am. Chem. Soc.* **2010,** *132*, 967-979. (b) Zeidan, T.; Manoharan,

M.; Alabugin, I. V. Ortho effect in the bergman cyclization: Interception of p-Benzyne intermediate by intramolecular hydrogen abstraction. *J. Org. Chem.* **2006**, *71,* 954-961.

12. Breiner, B.; Schlatterer, J. C.; Kovalenko, S. V.; Greenbaum, N. L.; Alabugin I. V. Protected 32P-labels in deoxyribonucleotides: Investigation of sequence selectivity of DNA photocleavage by Enediyne-, Fulvene-, and Acetylene-Lysine Conjugates. *Angew. Chem., Int. Ed*. **2006**, *45*, 3666-3670.

13. Yang, W.-Y.; Breiner, B.; Kovalenko, S. V.; Ben, C.; Singh, M.; LeGrand, S. N.; Sang, Q.-X. A.; Strouse, G. F.; Copland, J. A.; Alabugin, I. V. C-lysine conjugates: pH-controlled light-activated reagents for efficient double-stranded DNA cleavage with implications for cancer therapy. *J. Am. Chem. Soc.* **2009**, *131*, 11458-11470.

14. Koppenol, W. H.**;** Bounds, P. L.**;** DangOtto, C. V. Warburg's contributions to current concepts of cancer metabolism. *Nature Reviews Cancer* **2011**, *11*, 325-337.

15. Lyons, J. C.; Song, C. Killing of hypoxic cells by lowering the intracellular pH in combination with hyperthermia. *Radiat. Res.* **1995**, *141*, 216-218**.**

16 Song, C. W.; Lyons, J. C.; Griffin, R. J.; Makepeace, C. M. Thermosensitization by lowering intracellular pH with 5-(N-ethyl-N-isopropyl) amiloride. *Radiother. Oncol.* **1993**, *27*, 252-258.

17. Newell, K.; Wood, P.; Stratford, I.; Tannock, I. Effects of agents which inhibit the regulation of intracellular pH on murine solid tumours. *Br. J. Cancer* **1992**, *66*, 311-317.

18. Tannock, I. F.; Rotin, D. Acid pH in tumors and its potential for therapeutic exploitation. *Cancer Res.* **1989**, *49*, 4373-4384.

19. Stubbs, M.; Rodrigues, L.; Howe, F. A.; Wang, J.; Jeong. K. S.; Veech, R. L.; Griffiths, J. R. Metabolic consequences of a reversed pH gradient in rat tumors. *Cancer Res.* **1994**, *54*, 4011-4016.

20. Hatial, I.; Addy, P. S.; Ghosh, A. K.; Basak, A. Synthesis of highly efficient pH-sensitive DNA cleaving aminoethyl N-substituted cyclic enediyne and its L-Lysine conjugate. *Tetrahedron Lett*. **2013**, *54*, 854-857.

21. Kar, M.; Basak, A. Design, synthesis, and biological activity of unnatural enediynes and related analogues equipped with pH-dependent or phototriggering devices. *Chem. Rev.* **2007,** *107*, 2861-2890.

22. Breiner, B.; Kaya, K.; Roy, S.; Yang, W.-Y.; Alabugin, I. V. Hybrids of amino acids and acetylenic DNA-photocleavers: optimising efficiency and selectivity for cancer phototherapy. *Org. Biomol. Chem*. **2012**, *10,* 3974-3987.

23. Kovalenko, S. V., Alabugin, I. V. Lysine-Enediyne conjugates as photochemically triggered DNA double-strand cleavage agents. *Chem. Commun.* **2005**, *11*, 1444-1446.

24. Breiner, B.; Schlatterer, J. C.; Kovalenko, S. V.; Greenbaum, N. L.; Alabugin, I. V. DNA damage-site recognition by Lysine conjugates. *Proc. Natl. Acad. Sci. U. S. A.* **2007**, *104*, 13016-13021.

25. Yang, W.-Y.; Roy, S.; Phrathep, B.; Rengert, Z.; Kenworthy, R.; Zorio, D. A. R.; Alabugin, I. V. Engineering pH-Gated transitions for selective and efficient double strand DNA photocleavage in hypoxic tumors. *J.Med. Chem.* **2011**, 54, 8501-8506.

26. Yang, W.-Y.; Marrone, S. A.; Minors, N.; Zorio, D. A. R.; Alabugin, I. V. Insights into photochemistry responsible for the double-strand DNA-cleavage via structural perturbations in diaryl alkyne conjugates. *Beilstein. J. Org. Chem.* **2011**, *7,* 813–823.

27. Kaya, K.; Johnson, M.; Alabugin I. V. Opening enediyne scissors wider: pH-dependent DNA photocleavage by *meta*-diyne lysine conjugates. *Photochem. Photobiol.* **2015**, *91*, 748-758.

28. Yang, W.-Y.; Cao, Q.; Callahan, C.; Galvis, C.; Sang, A. Q.-X.; Alabugin, I. V. Intracellular DNA damage by lysine-acetylene conjugates. *J. Nucleic Acids* **2010**, Article ID 931394.

29. Gao, G.; DeRose, E. F.; Kirby, T. W.; London, R. E. NMR determination of lysine pKa values in the Pol lambda lyase domain: mechanistic implications. *Biochemistry* **2006**, *45*, 1785-1794.

30. To allow comparison of these pK_as with pK_as obtained by other methods, one has to take into account the difference between pK_aH*, which is obtained by a direct reading of the H_2O-calibrated pH meter in a D_2O solution, and pK_a (pK_a = 0.929pK_aH* + 0.42). pK_a values measured with pH* are assumed to be similar to the corresponding values in H_2O: Primrose, W. U. *NMR of Macromolecules. A Practical Approach*; Poberts, G. C. K., Ed., Oxford University Press: Oxford, **1993**, pp 22-23.

31. Kalsbeck, W.A.; Thorp, H.H. Determining binding constants of metal complexes to DNA by quenching of the emission of Pt2(pop)44- (pop = P205H22-). *J. Am. Chem. Soc.* **1993**, *115*, 7146-7151.

32. Sartorius, J.; Schneider, H.-J. Intercalation mechanisms with ds-DNA: binding modes and energy contributions with benzene, naphthalene, quinolone and indole derivatives including some antimalarials. *J. Chem. Soc. Perkin Trans. 2* **1997**, 2319-2327.

33. Freifelder, D.; Trubo, B. Matching of single-strand breaks to double-strand breaks in DNA. *Biopolymers*, **1969**, 7, 681-693.

34. Povirk, L. F.; Houlgrave, C. W. Effect of apurinic/apyrimidinic endonucleases and polyamines on DNA treated with bleomycin and neocarzinostatin: specific formation and cleavage of closely opposed lesions in complementary strands. *Biochemistry* **1988**, *27*, 3850-3857.

35. Hiraku, Y.; Ito, K.; Hirakawa, K.; Kawanashi, S. Photosensitized DNA damage and its protection via a novel mechanism. *Photochemistry and Photobiology* **2007**, *83*, 205-212.

36. (a) Steenken, S., Purine bases, nucleosides, and nucleotides: aqueous solution redox chemistry and transformation reactions of their radical cations and e- and OH adducts, *Chem. Rev*. **1989**, *89*, 503-520. (b) Dunn, D. A.; Lin, V. H.; Kochevar, I. E. Base-selective oxidation and cleavage of DNA by photochemical cosensitized electron transfer,*Biochemistry* **1992**, *31*, 11620-11625. (c) Sugiyama, H.; Tsutsumi, K.; Fujimoto, K.; Saito, I. Photoinduced deoxyribose C2' oxidation in DNA. Alkali-dependent cleavage of erythrose-containing sites via a retroaldol reaction, *J. Am. Chem. Soc.* **1993**, *115*, 4443-4448. (d) Cadet, J.; Berger, M.; Bunchko, G. W.; Joshi, R. C.; Raoul, S.; Ravanet, J.-L., 2,2-Diamino-4-[(3,5-di-O-acetyl-2-deoxy-.beta.-D-erythro- pentofuranosyl)amino]-5-(2H)-oxazolone: a novel and predominant radical oxidation product of 3',5'-Di-O-acetyl-2'-deoxyguanosine, *J. Am. Chem. Soc.* **1994**, *116*, 7403-7404. (e) Armitage, B.; Changjun, Y.; Devadoss, C.; Schuster, G. B., Cationic anthraquinone derivatives as catalytic DNA photonucleases: mechanisms for DNA damage and quinone recycling, *J. Am. Chem. Soc.* **1994**, *116*, 9847-9859.

37. Saito, I. Photochemistry of highly organized biomolecules: Sequence-selective photoreaction of DNA. *Pure Appl. Chem.* **1992**, *64*, 1305-1310.

38. Quadda, J. C.; Levy, M. J.; Hecht, S. M. Highly efficient DNA strand scission by photoactivated chlorobithiazoles. *J. Am. Chem. Soc.* **1993**, *115*, 12171-12172.

39. (a) Banerjee, J. A.; Yang, W.; Karplus, M.; Verdine, G. L. Structure of a repair enzyme interrogating undamaged DNA elucidates recognition of damaged DNA, *Nature* **2005**, *434*, 612-618. (b) Bruner, S. D.; Norman, D. P. G.; Verdine, G. L. Structural basis for recognition and repair of the endogenous mutagen 8-oxoguanine in DNA, *Nature* **2000**, *403*, 859-866. (c) Dodson, M. L.; Schrock III, R. D.; Lloyd, R. S., Evidence for an imino intermediate in the T4 endonuclease V reaction, *Biochemistry* **1993**, *32*, 8284-8290. (d) Dodson, M. L.; Michaels, M. L.; Lloyd, R.S., Unified catalytic mechanism for DNA glycosylases, *J. Biol. Chem.* **1994**, *269*, 32709-32712. (e) Faucher, F.; Wallace, S. S.; Doublié, S. The C-terminal lysine of Ogg2 DNA glycosylases is a major molecular determinant for guanine/8-oxoguanine distinction, *J. Mol. Biol.* **2010**, *397*, 46-56. (f) Similar reactivity of lysine in nucleosome core particle: (g) Sczepanski, T.; Wong, R. S.; McKnight, J. N.; Bowman, G. D.; Greenberg, M. M. Rapid DNA–protein cross-linking and strand scission by an abasic site in a nucleosome core particle, *Proc. Natl. Acad. Sci. U.S.A* **2010**, *107*, 22475-22480.

40. Yoshimura, Y.; Inomata, T.; Nakazawa, H.; Kubo, H.; Yamaguchi, F.; Ariga, T. Evaluation of free radical scavenging activities of antioxidants with an H(2)O(2)/NaOH/DMSO system by electron spin resonance. *J. Agric. Food Chem*. **1999**, *47*, 4653-4656:

41. Rosenblum, W. L.; El-Sabban, F. Dimethyl sulfoxide (DMSO) and glycerol, hydroxyl radical scavengers, impair platelet aggregation within and eliminate the accompanying vasodilation of, injured mouse pial arterioles. *Stroke* **1982**, *13*, 35-39.

42. Devasagayam, T.P.A.; Steenken, S.; Obendorf, M.S.W.; Schulz, W.A.; Sies, H. Formation of 8-hydroxy(deoxy)guanosine and generation of strand breaks at guanine residues in DNA by singlet oxygen. *Biochemistry* **1991**, *30*, 6283-6289.

43. Lindahl, T.; Nyberg, B. Rate of depurination of native deoxyribonucleic acid. *Biochemistry* **1972**, *11*, 3610–3618.

44. Boiteux, S.; Guillet, M. Abasic sites in DNA: repair and biological consequences in *Saccharomyces cerevisiae*. *DNA Repair* **2004**, *3*, 1-12.

45. Rydberg, B.; Lindahl, T. Nonenzymatic methylation of DNA by the intracellular methyl group donor S-adenosyl-l-methionine is a potentially mutagenic reaction. *The EMBO Journal,* **1982**, *1*, 211–216

46. Lindahl, T.; Nyberg, B. Heat-induced deamination of cytosine residues in deoxyribonucleic acid. *Biochemistry* **1974**, *13*, 3405–3410.

47. Cadet, J.; Berger, M.; Douki, T.; Ravanat, J. L. Oxidative damage to DNA: formation, measurement, and biological significance. *Rev. Physiol. Biochem. Pharmacol*. **1997**, *131*, 1–87.

Tables

Table 1. Summary of pK_a values of the compounds.

Fluorescence	**1**	**2**	**3**	**4**	**5**	**6**	**7**	**8**
pKa 1	7.3	7.3	7.3	7.0	6.6	7.1	5.5	6.3
pKa 2	-	-	-	-	-	-	8.1	7.8
^{1}H NMR								
pKa 1	7.3	6.6	-	7.2	7.0	7.2	-	-
pKa 2	7.4	6.7	-	7.7	7.8	-	-	-

Table 2. DNA Binding constants from UV

	K_b(**1**)	K_b(**2**)	K_b(**3**)	K_b(**4**)	K_b(**5**)	K_b(**6**)	K_b(**7**)	K_b(**8**)
pH 6	$2.89*10^4$	$1.17*10^5$	$1.04*10^5$	$2.83*10^4$	$4.44*10^4$	$1.07*10^5$	$5.85*10^4$	$2.23*10^5$
pH 7	$8.89*10^4$	$1.31*10^5$	$1.68*10^5$	$1.05*10^5$	$6.75*10^4$	$1.27*10^5$	$1.50*10^5$	$1.46*10^5$
pH 8	$3.03*10^5$	$6.67*10^5$	$1.80*10^5$	$1.50*10^5$	$2.02*10^5$	$3.21*10^5$	$2.05*10^5$	$2.33*10^5$

Table 3. Stern-Volmer quenching constants of the compounds (**1**-**8**) from EtBr displacement.

	K_{SV}(**1**)	K_{SV}(**2**)	K_{SV}(**3**)	K_{SV}(**4**)	K_{SV}(**5**)	K_{SV}(**6**)	K_{SV}(**7**)	K_{SV}(**8**)
pH 6	6.8	27.8	26.0	7.0	11.1	27.8	9.0	9.4
pH 7	5.7	9.2	9.2	4.4	7.8	23.6	4.9	5.9
pH 8	3.4	6.7	5.7	1.5	5.2	6.3	3.1	2.6

Table 4. Statistical analysis of the single-strand and double-strand break formation by **1**, **2** and **3** as a function of irradiation time at pH 6.0.

	Number of ss-breaks (n_1) and ds-breaks (n_2) per molecule **1** at pH 6			Random	Random
Time/min	n_1	n_2	**n_1/n_2**	Expected n_2	n_1/n_2
4.0	0.6	0.07	9.4	0.00073	853
6.0	1.7	0.19	9.1	0.00553	309
8.0	1.9	0.29	6.6	0.00712	273
	Number of ss-breaks (n_1) and ds-breaks (n_2) per molecule **2** at pH 6			Random	Random
Time/min	n_1	n_2	**n_1/n_2**	Expected n_2	n_1/n_2
4.0	0.7	0.00	-	0.00106	705
6.0	1.0	0.13	8.04	0.00201	513
8.0	1.7	0.21	8.0	0.00528	317
	Number of ss-breaks (n_1) and ds-breaks (n_2) per molecule **3** at pH 6			Random	Random
Time/min	n_1	n_2	**n_1/n_2**	Expected n_2	n_1/n_2
4.0	0.7	0.00	-	0.00087	778
6.0	0.8	0.15	5.3	0.00115	678
8.0	0.9	0.20	4.3	0.00140	615

Schemes

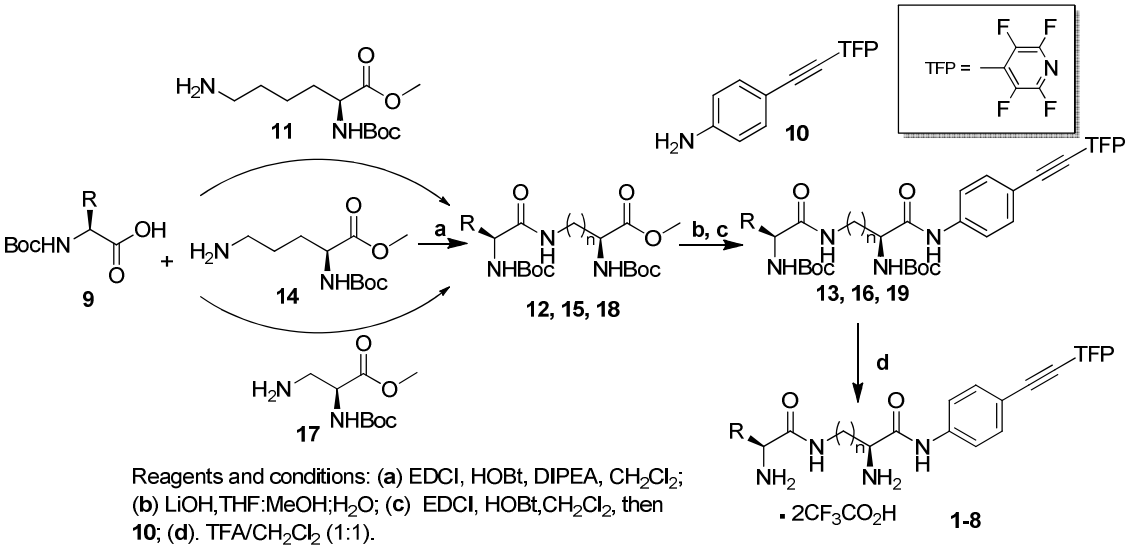

Scheme 1. Synthesis of designed hybrid molecules.

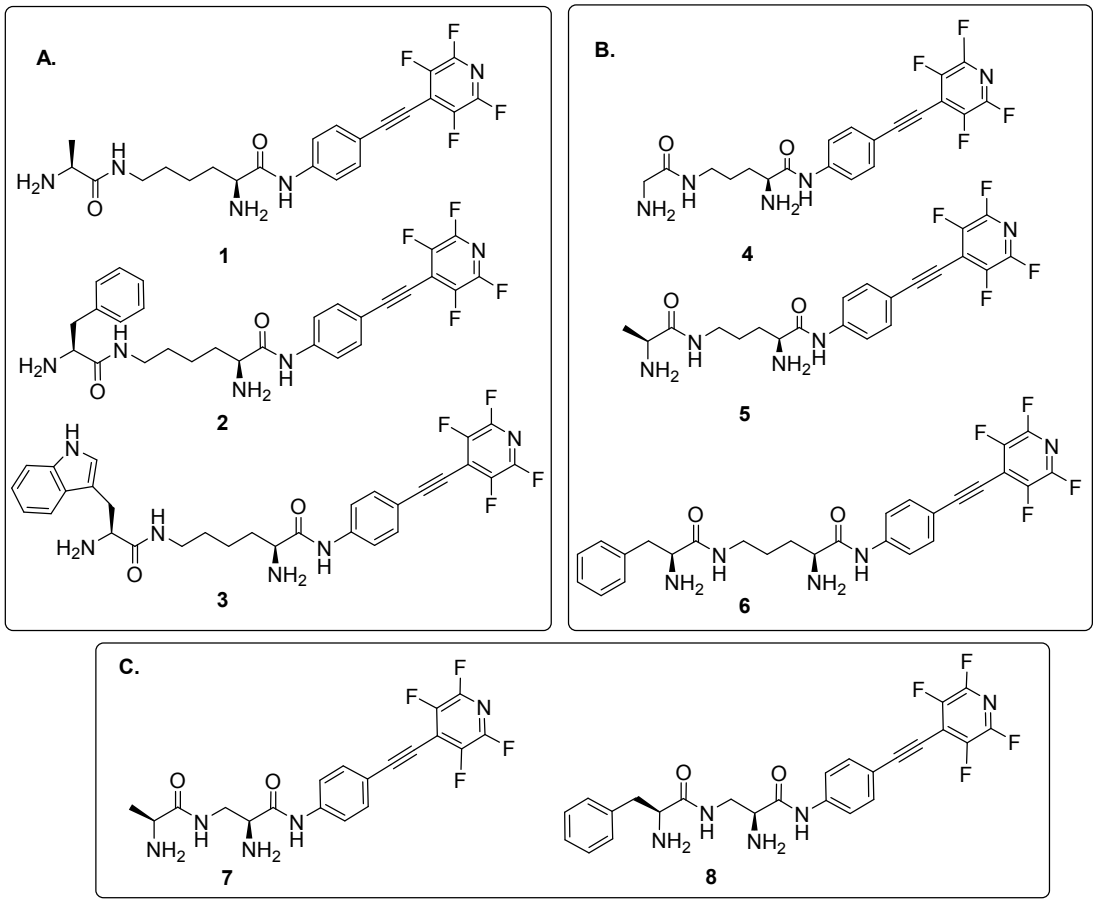

Scheme 2. The structures of dipeptide-acetylene conjugates. A: Lysine bridge. B: Ornithine bridge. C: **α** -Amino alanine bridge.

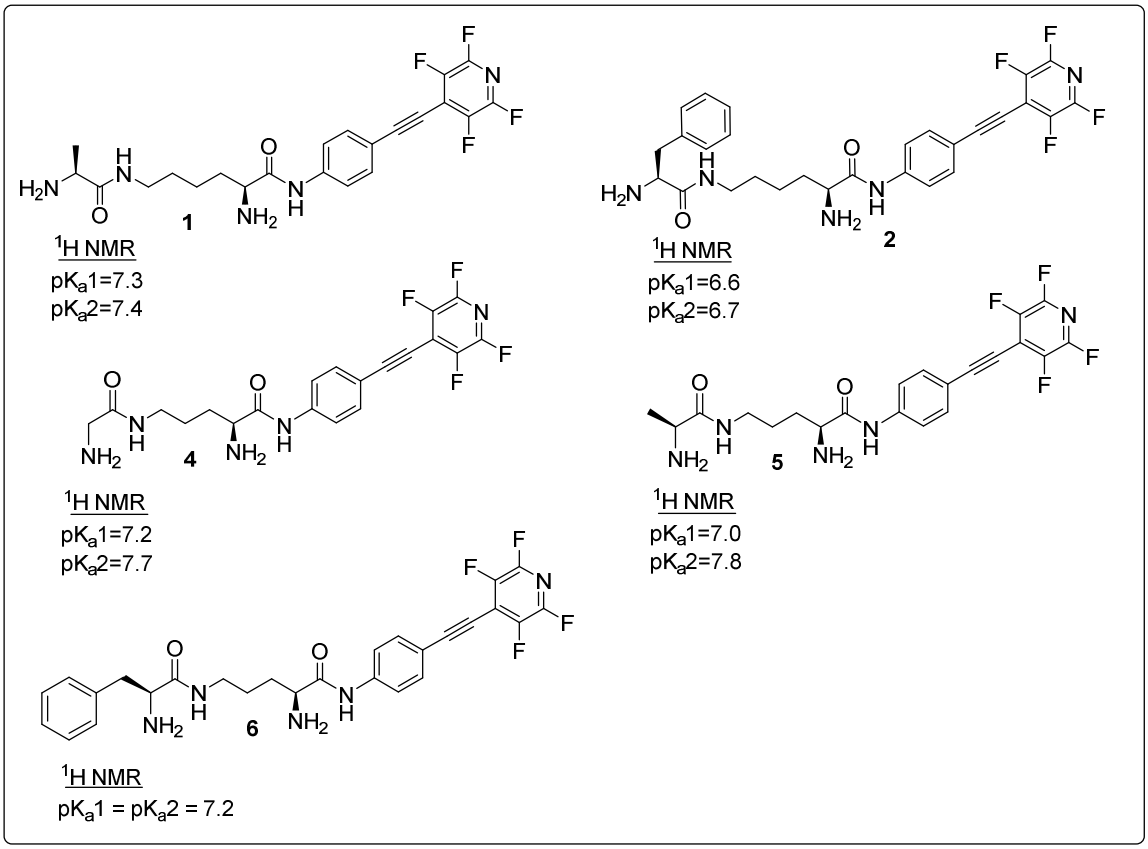

Scheme 3. The pK$_a$ values obtained from ^{1}H NMR titration.

Figures

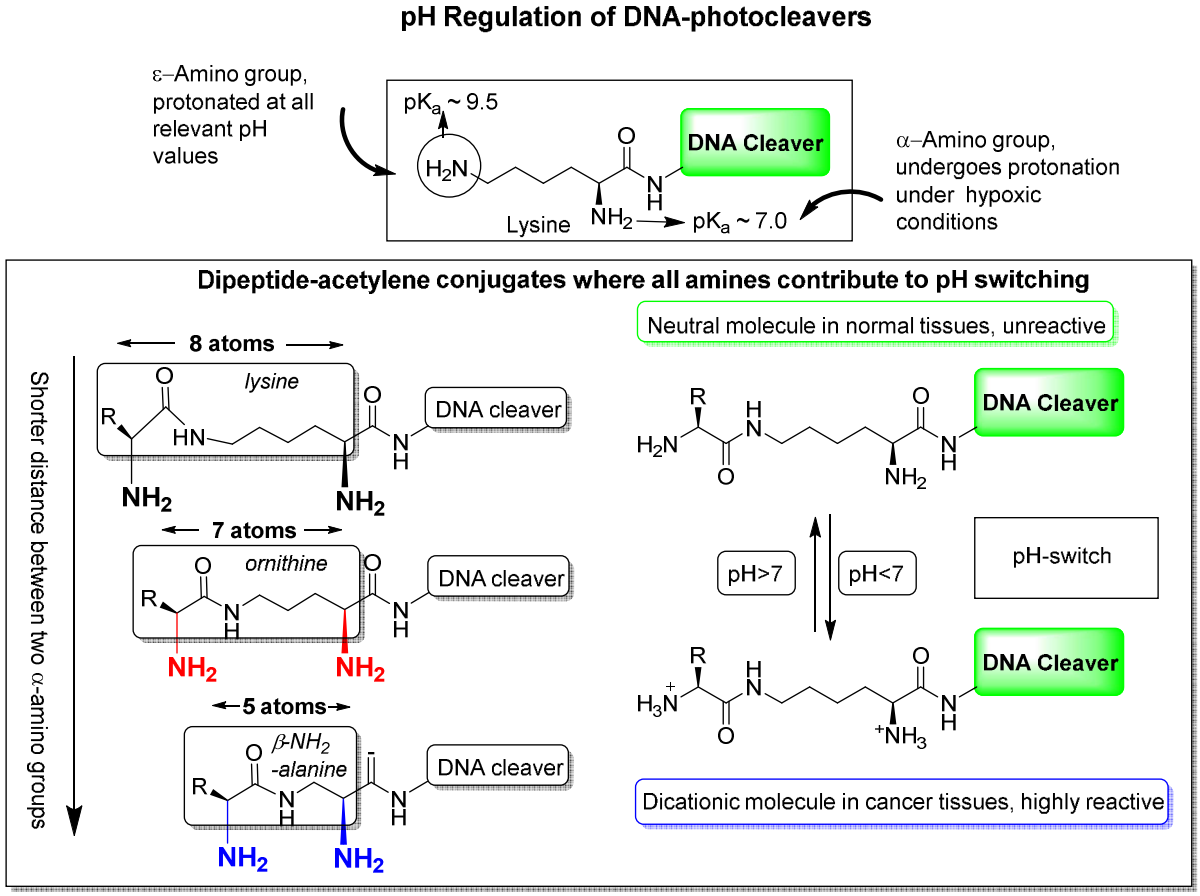

Figure 1: Left: Design of new amino acid-acetylene hybrids with variable distances between the two α-NH2 groups. Right: the concept of pH-regulation of the DNA-cleaving activity of light-activated DNA cleaving agents.

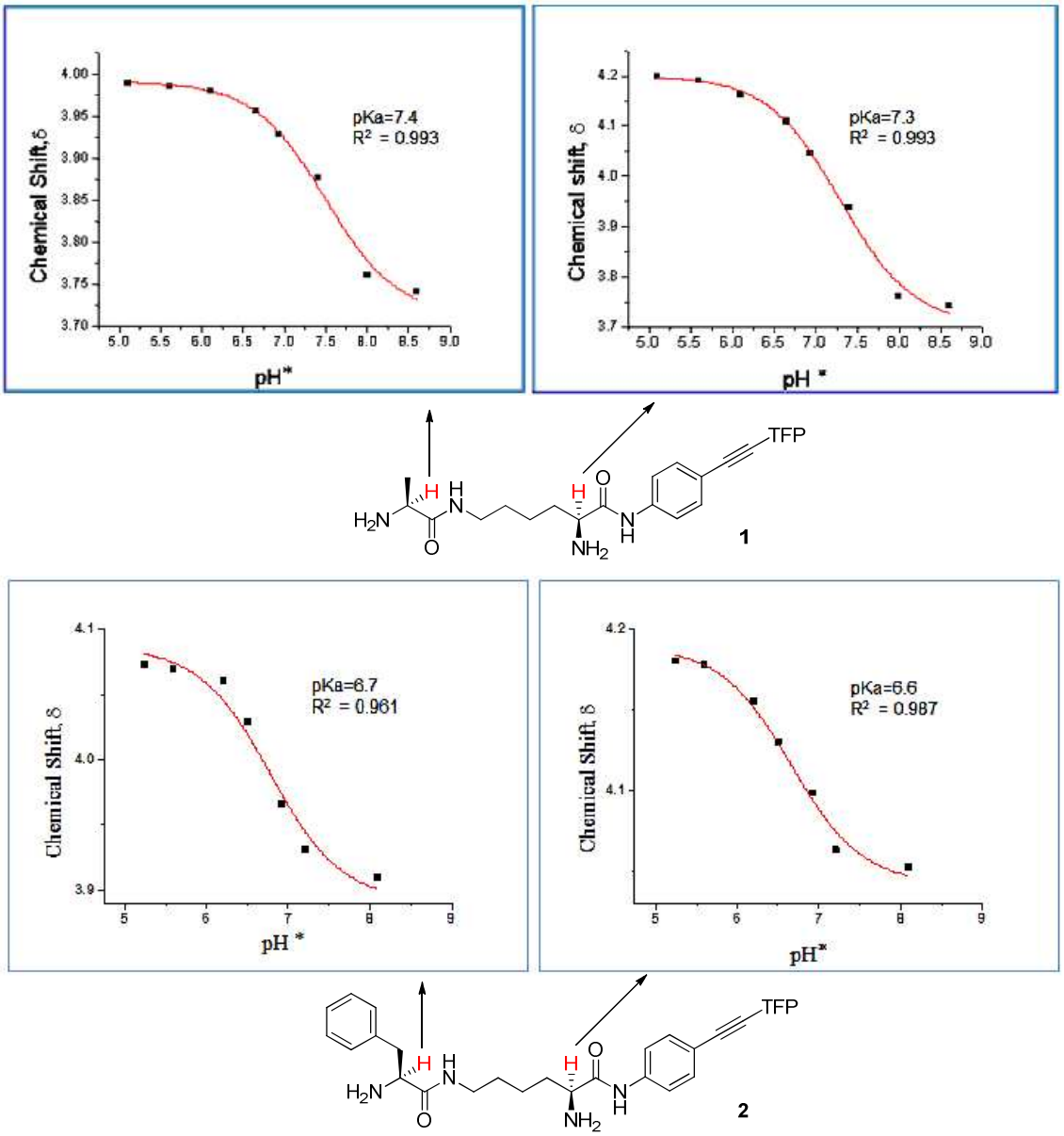

Figure 2. Chemical shift-pD titration plots for α-hydrogens in conjugates **2** and **3** (1 mM) in D_2O.

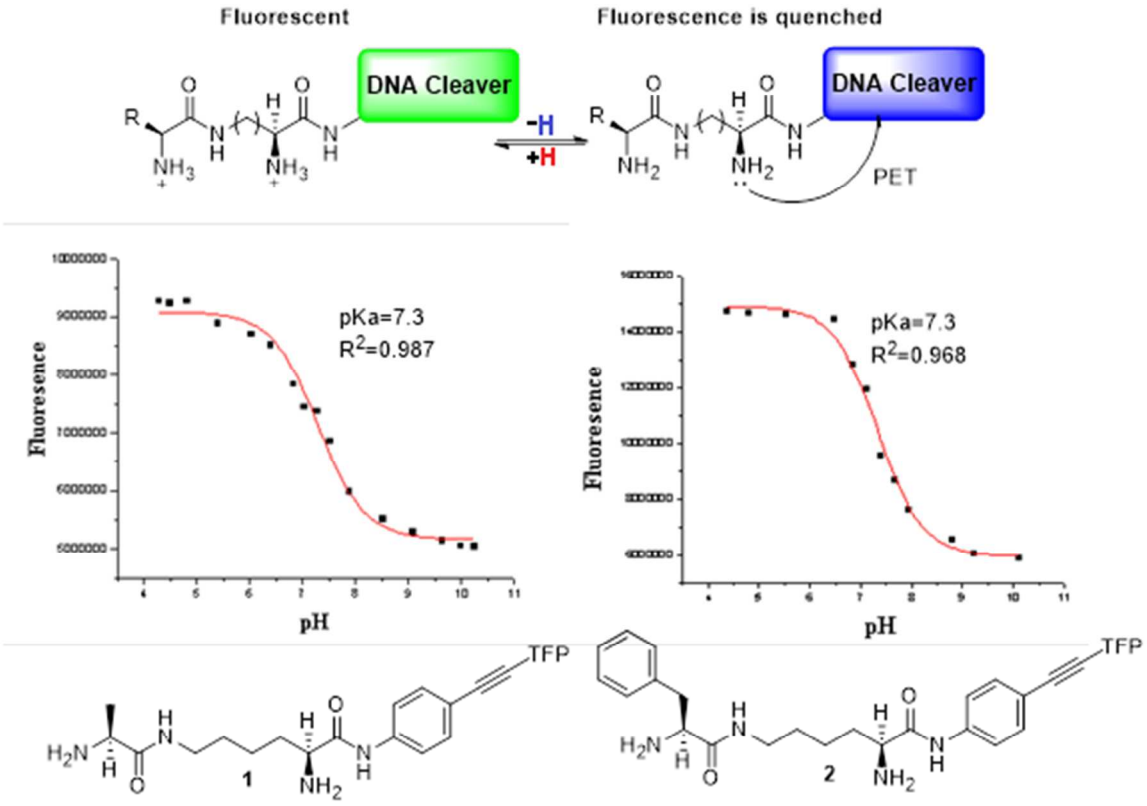

Figure 3. Selected pKa values obtained from fluorescence.

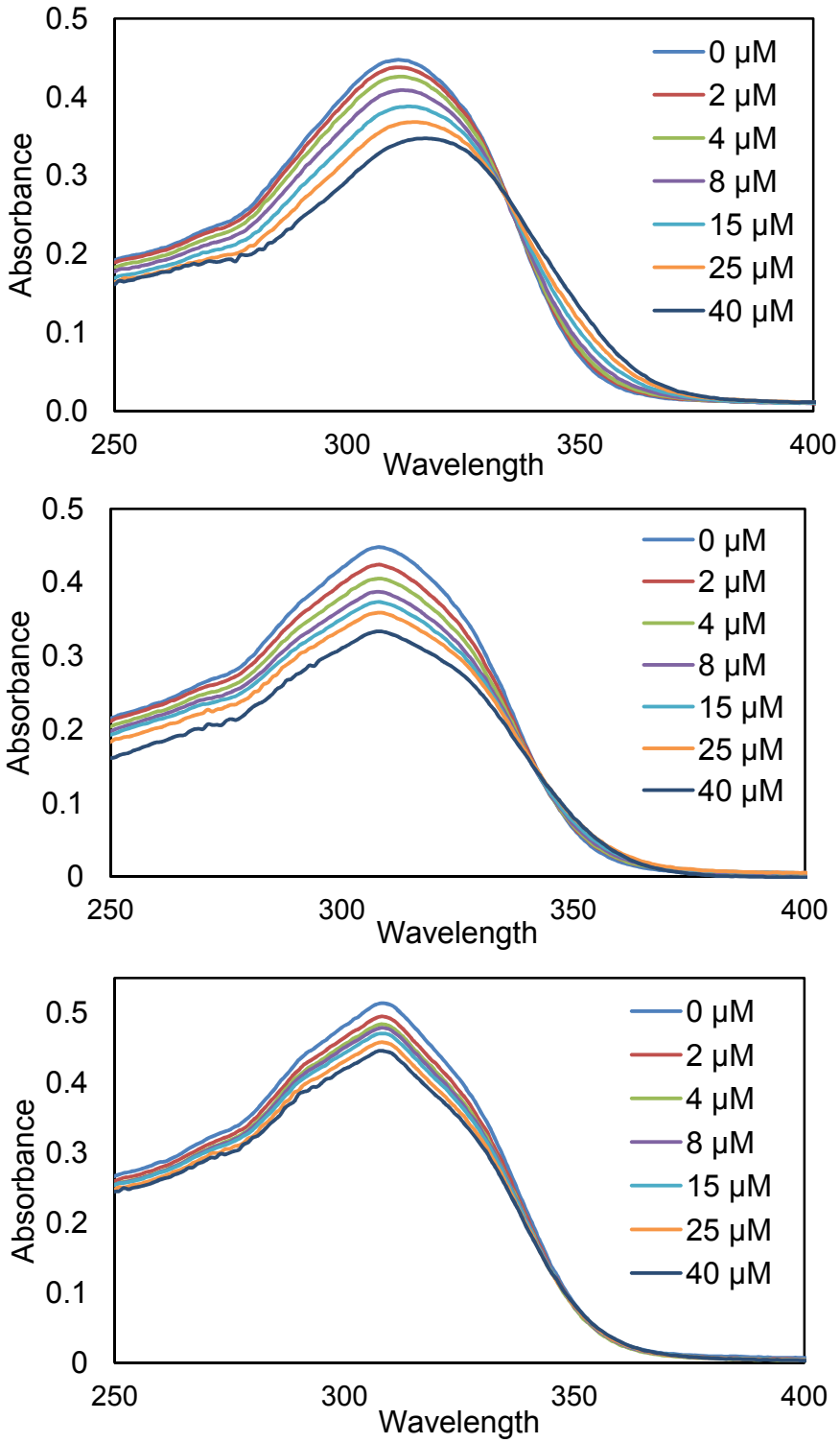

Figure 4. Absorption spectral changes of **1** (15 μM) on titration of CT DNA (0– 40 μM) in phosphate buffer (pH 6, pH 7 and pH 8).

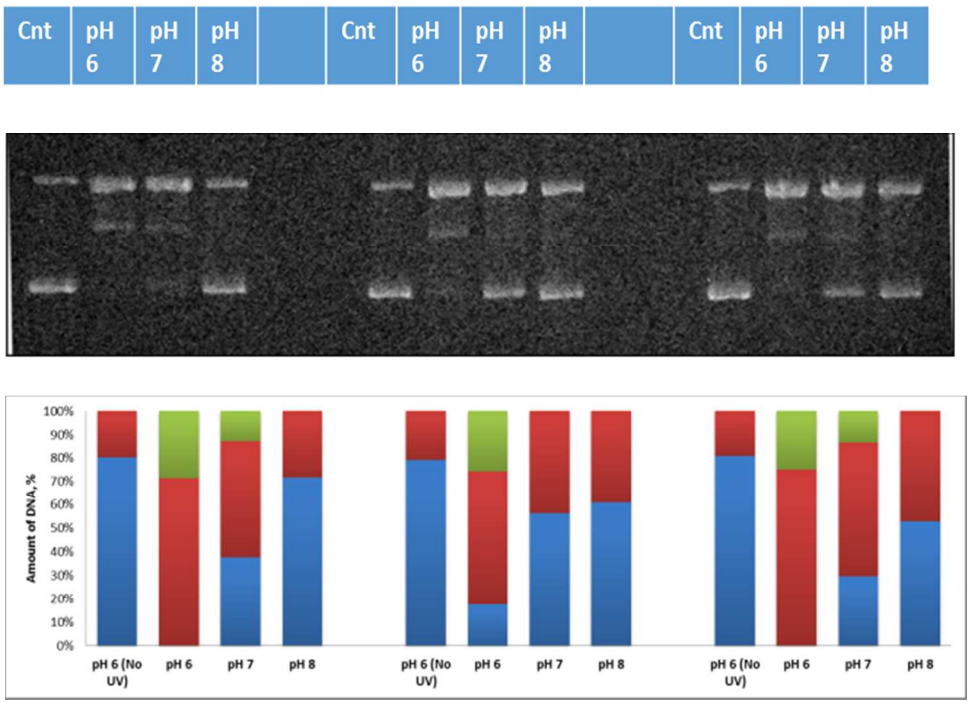

Figure 5. Quantified cleavage data for plasmid relaxation assay for DNA photocleavage with 15 μM of acetylenic conjugates **1** (left), **2** (middle), **3** (right) and 38 μM (b.p.) of pBR322 plasmid DNA at pH range of 6 – 8 after 10 min. of UV (>300 nm) irradiation. Reported values represent the average of three experiments. Code: Form I, Blue; Form II, Red; Form III, Green.

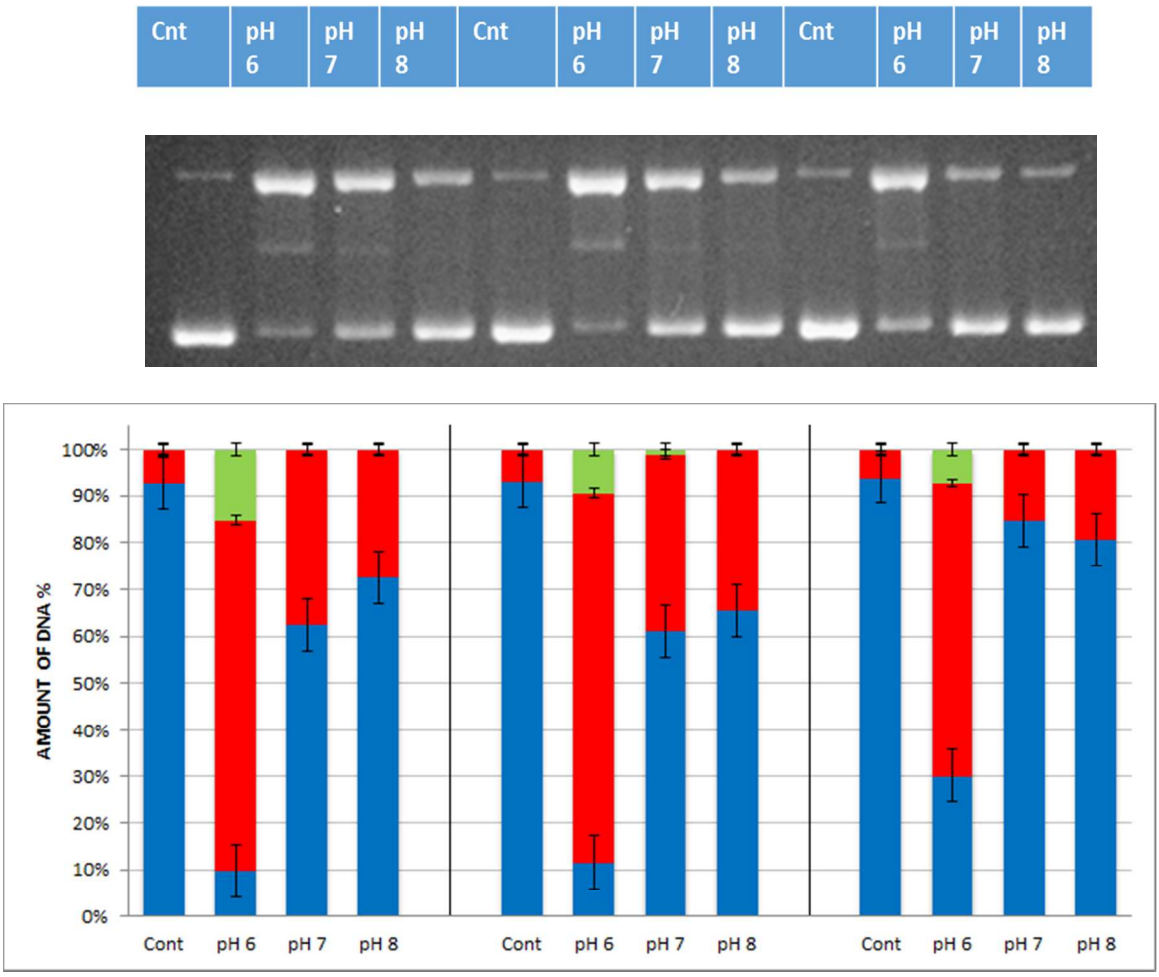

Figure 6. Quantified cleavage data for plasmid relaxation assay for DNA photocleavage with 15 μM of acetylenic conjugates **4** (left), **5** (middle), **6** (right) and 38 μM (b.p.) of pBR322 plasmid DNA at pH range of 6 – 8 after 10 min. of UV (>300 nm) irradiation. Reported values represent the average of three experiments. Code: Form I, Blue; Form II, Red; Form III, Green.

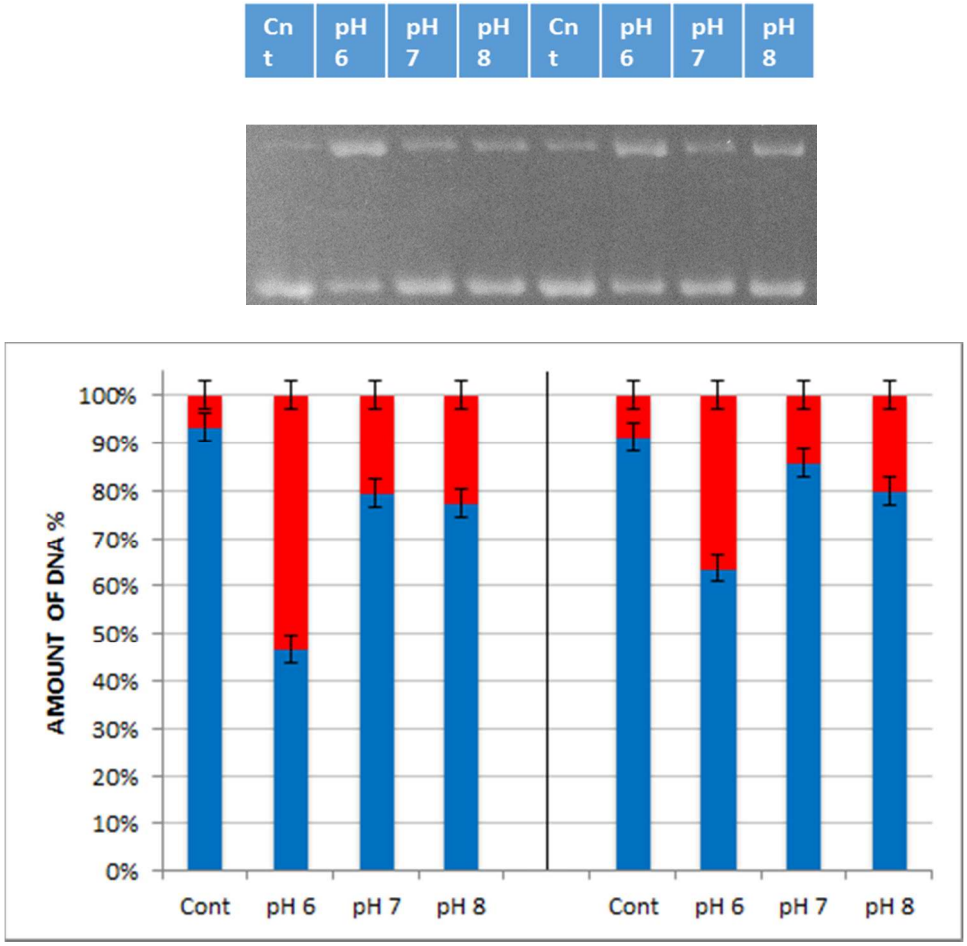

Figure 7. Quantified cleavage data for plasmid relaxation assay for DNA photocleavage with 15 μM of acetylenic conjugates **7** (left) and **8** (right) and 30 μM (b.p.) of pBR322 plasmid DNA at pH range of 6 – 8 after 10 min. of UV (>300 nm) irradiation. Reported values represent the average of three experiments. Code: Form I, Blue; Form II, Red.

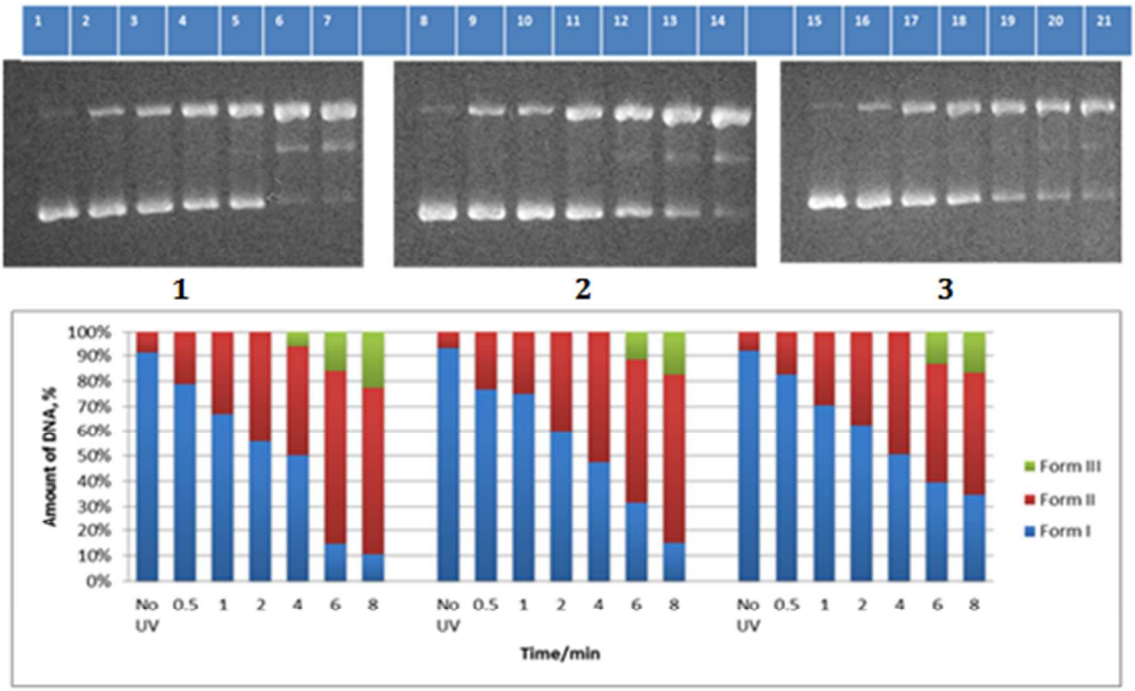

Figure 8. Quantified cleavage data for plasmid relaxation assay for DNA photocleavage with 15 μM of conjugates **1** (left), **2** (middle), **3** (right) and 30 μM (b.p.) of pBR322 plasmid DNA at pH range of 6 – 8 after 10 min. of UV (>300 nm) irradiation. Code: Form I, Blue; Form II, Red; Form III, Green

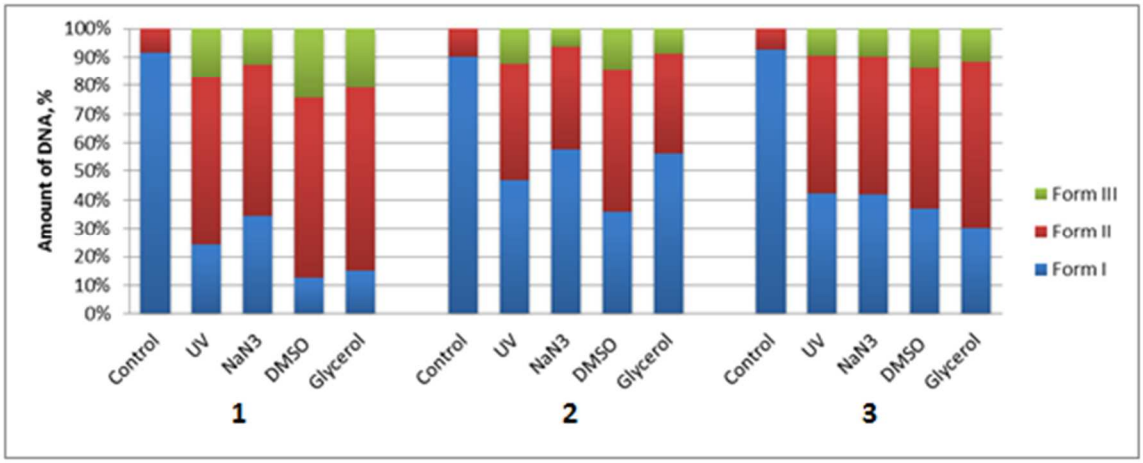

Figure 9. Effect of hydroxyl radical/singlet oxygen scavengers (20 mM) upon the efficiency of DNA cleavage of compounds **1** (left), **2** (middle) and **3** (right) at pH 6 at 15 μM of compounds.

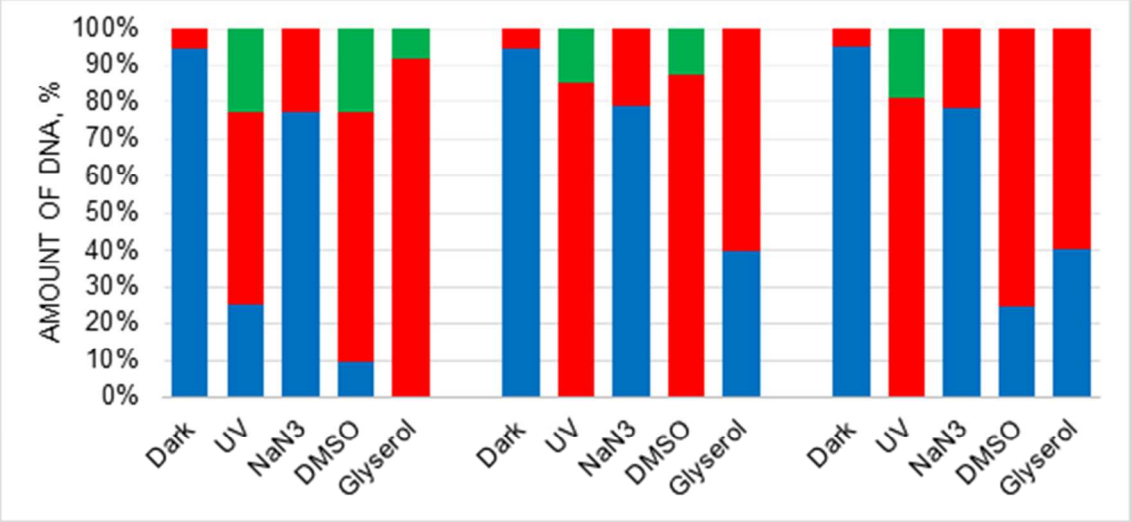

Figure 10. Effect of hydroxyl radical/singlet oxygen scavengers (20 mM) upon the efficiency of DNA (30 μM b.p.) cleavage of compounds **4** (left), **5** (middle) and **6** (right) at pH 6 (20mM sodium phosphate buffer) at 15 μM of compounds.

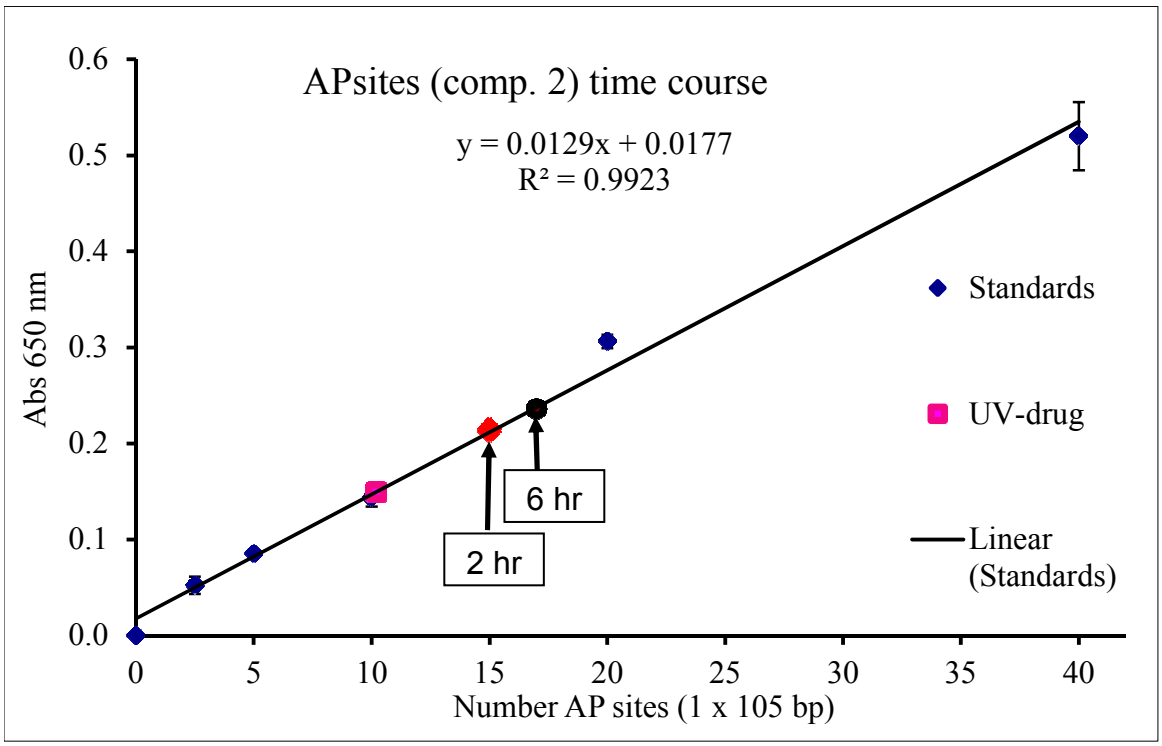

Figure 11. Abasic Site Generation/Detection by the compound **2**.

Table of Contents Graphics